Supplemental Material

Frataxin deficiency promotes endothelial senescence in pulmonary hypertension

Miranda K. Culley, Jingsi Zhao, Yi Yin Tai, Ying Tang, Dror Perk, Vinny Negi, Qiujun Yu, Chen-Shan C. Woodcock, Adam Handen, Gil Speyer, Seungchan Kim, Yen-Chun (Charly) Lai, Taijyu Satoh, Annie Watson, Yassmin Al Aaraj, John Sembrat, Mauricio Rojas, Dmitry Goncharov, Elena A. Goncharova, Omar F. Khan, Daniel G. Anderson, James E. Dahlman, Aditi Gurkar, Robert Lafyatis, Ahmed U. Fayyaz, Margaret M. Redfield, Mark T. Gladwin, Marlene Rabinovitch, Mingxia Gu, Thomas Bertero, Stephen Y. Chan

Supplemental Methods

Cell culture

Primary human pulmonary artery endothelial cells (PAECs) (Lonza; 58-year-old male and 38-year-old female donors) as well as smooth muscle cells (PASMCs) (ThermoFisher) and adventitial fibroblasts (PAAFs) (ThermoFisher) were cultured in cell-specific basal media supplemented with growth media kit (PromoCell; Lonza) and 5% fetal bovine serum (FBS) without antibiotics or antifungals added. Experiments were performed between passages 4 and 9. Pulmonary microvascular endothelial cells (PMVECs) from a Group 1 PAH patient (male, 35 years old) were compared to a no PH control (male, 31 years old) (from D. Goncharov and E.A. Goncharova). Cell isolation from manual dissection of lung parenchyma followed by characterization and maintenance were performed as described (1). Inducible pluripotent stem cells from FRDA patients (NIGMS Human Genetic Cell Repository at the Coriell Institute for Medical Research; GM23404, GM23913) (2) and healthy controls (from M. Gu and M. Rabinovitch) were differentiated into endothelial cells (3), grown in endothelial basal growth media (PromoCell) containing 20% FBS, and used for study between passages 2 and 8. Serum-starved primary cells were exposed to hypoxia (0.2% O_2, 5% CO_2, with N_2 balance) using a modular hypoxia chamber or standard non-hypoxic conditions (21% O_2), recombinant IL-1β (R&D Systems, 10ng/ml), recombinant IL6/IL6R alpha (R&D Systems, 10ng/ml), cobalt(II) chloride (Sigma Aldrich, 750µM), and ABT-263 (Sellekchem, 0.25µM) or exposed to soft (0.5 kPa) versus stiff matrix (50 kPa) (Matrigen) (4) for ≥ 24 hours.

RNA extraction and quantitative RT-PCR

Cells were lysed in Qiazol (Qiagen) and RNA extracted using Rneasy Mini Kit (Qiagen), according to the manufacturer's instructions. Complementary DNA (cDNA) synthesis was performed using the reverse transcription kit per the manufacturer's instructions (ThermoFisher) on an Applied Biosystems Real Time PCR instrument (ThermoFisher). Quantitative RT-PCR (RT-qPCR) was performed on an Applied Biosystems QuantStudio 6 Flex Fast Real Time PCR device, and fold-change of RNA species was calculated using the formula ($2^{-\Delta\Delta Ct}$) normalized to β-actin or SIN3A expression. TaqMan primers were purchased from ThermoFisher and are listed in **Supplemental Table 7**.

Immunoblotting

Cells were lysed in RIPA buffer (ThermoFisher) with added protease inhibitor (Thermofisher) and phosphatase inhibitor (PhosSTOP, Roche), and the concentration of the soluble protein fraction was estimated using a Pierce BCA protein assay kit (ThermoFisher). Protein lysates (15-20μg) were separated by a 4-15% gradient SDS-PAGE gel system (Biorad) and transferred onto a PVDF membrane (ThermoFisher). Membranes were blocked in 5% non-fat milk in Phosphate-Buffered Saline (PBST) or BSA in Tris-buffered Saline with 0.1% Tween20 (TBST) for 1 hour at room temperature and incubated with primary antibodies at 4 degrees C overnight. A complete summary of primary antibodies is listed in **Supplemental Table 8**. After washing with PBST or TBST (≥10 minutes, three times), membranes were exposed to appropriate secondary antibodies (anti-rabbit, anti-mouse, and anti-rat) coupled to HRP (Dako) for 1 hour at room temperature. After another set of washes, immunoreactive bands were visualized with the Pierce ECL reagents (ThermoFisher) and Biorad ChemiDoc XRS+ and ImageLab 6.0.1 software. Densitometry was quantified using the NIH ImageJ software (http://rsb.info.nih.gov/ij/).

Senescence-associated β-galactosidase staining

Transfected PAECs or iPSC-ECs at <80% confluency were washed with PBS twice and then PFA-fixed for 10 minutes at room temperature before staining with the Senescence β-galactosidase Staining Kit (Cell Signaling Technology) overnight at 37 degrees C in a dry incubator. After 12-18 hours incubation, images were taken using EVOS XL CORE imaging system (Life Technologies) with a 10x magnification and SA-β-gal staining was quantified using NIH ImageJ software (http://rsb.info.nih.gov/ij/).

Transfection

PAECs and PASMCs were plated in collagen-coated plastic and cultured to 70-80% confluency. Transfection was performed using pre-determined siRNA concentrations and Lipofectamine 2000 reagent (Life Technologies) in one-part OptiMEM (ThermoFisher) and three-parts serum-starved cell specific media (PromoCell). Following 6-8 hours incubation, transfection media was removed and replaced with full serum cell-specific growth media. Experiments were performed 48 hours post-transfection unless otherwise specified. Silencer Select siRNAs for BMPR2 (s2044), ENG (s4678), CAV1 (s2447), ACRVL1 (s502493), EIF2AK4 (s532694), HIF-1α (s6541), HIF-2α (s4699), CTCF (s20967), BRD2 (s12070), BRD4 (s23901), HDAC1 (s75), HDAC3 (s16876), and negative control #1 and #2 were purchased from Life Technologies. FXN (sc-40580) as well as two negative control (sc-37007, sc-44236) pooled siRNAs were purchased from Santa Cruz.

Plasmid construction and lentivirus production

The coding sequence of FXN transcript 1 (mitochondrial isoform; Dharmacon, clone ID 4829356) and ISCU1 (cytosolic isoform; clone ID: 23479) and 2 (mitochondrial isoform; clone ID 66383) were purchased and sub-cloned in the pCDH-CMV-MCS-EF1-copGFP (System Biosciences #CD511B-1) using EcoRI and NotI restriction sites, respectively. HEK293T cells (American Type Culture Collection) were grown in DMEM containing 10% FBS and transfected using Lipofectamine 2000 (Life Technologies) with lentiviral plasmids along with a packaging plasmid system (pPACK, System Biosciences), according to the manufacturer's instructions. Viral particles were harvested 60 hours after transfection, concentrated, and sterile filtered (0.45 µm). Transduction was performed in cultured PAECs (70-80% confluence) by incubating lentiviral vectors compared to a parent vector expressing GFP and polybrene (8 μg/ml) in serum- and antibiotic-free cell-specific media for 60 hours. Experiments were performed 72 hours after infection. Transduction efficiency was assessed in each experiment by observing the GFP expression under a fluorescence microscope and assessing expression of lentiviral targets by RT-qPCR.

Fe-S fluorescent sensor

Expression plasmids for GRX2 and GCN4 transgenes fused to the N-terminal or C-terminal portions of the Venus fluorescent protein were generously provided by Dr. J. Silberg (Rice University), as previously described (5, 6). Transgenes were subcloned into the pCDH-MCS-EF1-PURO lentiviral parent vector (System Biosciences) via BamHI and NotI sites. PAECs were transfected with FXN or control siRNAs as described above and then 24 hours later were transduced with Fe-S fluorescent sensor lentiviruses in the presence of 8μg/ml polybrene (Santa Cruz Biotechnology). Fluorescence was imaged by an EVOS FL microscope (Life Technologies), and Fe-S content was presented as percentage of PAECs with positive fluorescence. Manual quantification was performed blinded.

RNA sequencing and gene set enrichment analysis

<u>Single cell RNA sequencing:</u> Using previously published single cell RNA sequencing data from Group 1 PAH lungs compared to non-PH controls (n=3/group) (7), expression matrices were derived using CellRanger (8). Batch correction, scaling, and normalizing were all performed using SCTransform in Seurat v3 (9-11). Cell types were determined with SingleR (12) using the Blueprint ENCODE reference (13, 14). Cells were identified as positively expressing $p16^{INK4}$ or FXN if the transformed expression value was greater than 0. Cells expressing Ki67 were identified as having a transformed expression value greater than 0.2.

Long RNA sequencing: Separately, following total RNA extraction from transfected PAECs and Broad Range RNA Qubit quality control and long RNA sequencing (Paired-end read 75 cycles, 40-50M reads/sample) was run by the Health Sciences Sequencing Core (UPMC Children's Hospital of Pittsburgh). Transcript quantification was performed using Salmon and differential expression using DESEQ (15, 16). The complete data set is available in the GEO repository via the accession number GSE171692. Pathway enrichment of direct Gene Ontology biological processes was performed using DAVID version 6.8 (17-20) on genes with an absolute log fold change > 1.2 and FDR corrected p-value < 0.05 (**Supplemental Table 5**). The significant processes were then grouped into DNA replication, cellular response to DNA damage stimulus, and Cell cycle based on term ancestry. These were used to construct the hypergraph.

Cell cycle analysis

Cell cycle phase was determined using the BD Pharmingen BrdU Flow Kit. To summarize, transfected PAECs were serum-starved overnight and then pulsed with BrdU (10μM) in serum replete endothelial cell media for 4 hours at 37 degrees C. Cells were washed with PBS three times, trypsinized, and fixed for 30 minutes on ice. Following fixation, samples were washed, spun down, and the supernatant discarded before permeabilization for 10 minutes on ice. Following another wash step, PAECs were re-fixed for 5 minutes on ice before incubation with Dnase (300μg/ml) for 1 hour at 37 degrees C. After an additional wash step, cells were incubated with anti-BrdU antibody (1:50) for 20 minutes at room temperature, washed again, and ultimately stained with 7-amino-actinomycin D (7-AAD). Stained cells were gated based upon BrdU (FITC) and 7-AAD (PE-Texas Red-A, linear) following flow cytometry analysis (BD LSRFortessa and FlowJo).

Replication assays

BrdU Cell Proliferation Assay Kit (Cell Signaling Technology) was performed per the manufacturer's instructions with overnight serum-starvation to sync cell cycle prior to BrdU pulse. Colorimetric change (absorbance 450nm) was assessed by spectrophotometer. Separately, after serum-starvation overnight, transfected PAECs were exposed to serum-replete media for 4 hours, collected, and manually counted using a haemocytometer.

Apoptosis assays

The Caspase-Glo 3/7 Assay (Promega) was performed per the manufacturer's instructions and chemiluminescence was measured by spectrophotometer (Biotek). Results were normalized to protein concentration.

DNA fiber staining

DNA preparation, staining, and imaging was performed per the described protocol (21). Briefly, transfected PAECs were serum-starved overnight and then exposed to CldU (50μM) followed by IdU (250μM) for 10 minutes each in serum-replete media; plated cells were washed with PBS three times after each pulse. On a glass slide, PAECs resuspended in PBS (1200 cells/μl) were lysed with 0.5% SDS, 200mM Tris HCl, 50mM EDTA, pH 7.4 for 5 minutes at room temperature before allowing the mixed solution to spread across the slide surface by tilting the slide to a 15 degree angle. After drying, DNA was fixed with 3:1 Methanol: Acetic acid for 5 minutes and denatured with 2.5M HCl for 30 minutes at room temperature. After washing, samples were blocked with 0.1% Triton X-100 and 10% goat serum in PBS for 1 hour at 37 degrees C and incubated with primary antibodies (rat anti-BrdU, mouse anti-BrdU) overnight at 4 degrees C. After washing, slides were incubated for 1 hour at 37 degrees C with secondary antibodies (488-conjugated anti-rat, Cy3-conjugated anti-mouse) and mounted using gelvatol. Imaging was performed using a Nikon A1 confocal microscope and 60x oil immersion lens with 1.75x zoom.

Quantification was blinded and performed on >100 fibers/samples using NIH ImageJ software (http://rsb.info.nih.gov/ij/).

Proximity ligation assay

Endogenous interaction of the DNA Pol δ protein subunits (POLD1 and 3) was assessed using a Duolink Proximity Ligation Assay kit (Sigma Aldrich) per the manufacturer's instructions. Briefly, iPSC-ECs were plated in Lab-Tek II chamber slides (5000 cells/well), fixed with 4% paraformaldehyde for 15 minutes, permeabilized with 0.25% Triton X-100 for 15 minutes, and blocked for 30 minutes at 37 degrees C before incubation with primary antibodies overnight at 4 degrees C (1:250). After washing, fixed cells were exposed to PLUS and MINUS PLA probes for 1 hour, ligated for 30 minutes, and amplified with polymerase for 1 hour and 40 minutes all at 37 degrees C. Cells were counterstained and mounted with DAPI solution. Imaging was performed on a Nikon A1 microscope with 60x oil immersion objective at 1.75x zoom; >10 images were taken per sample. Quantification was blinded and performed manually.

Rodent models of PH

There was randomization of animals assigned to different experimental groups. Briefly, populations of animals sharing the same gender, genotype, and similar body weight were placed in one container. Then, each animal was picked randomly and assigned in a logical fashion to different groups. For example, the first one is assigned to group A, the second to group B, the third to group A, the fourth to group B, and so forth. No animals were excluded from analyses.

<u>Chronic hypoxia in mice:</u> 10-12 week-old C57BL/6 wild type mice (Taconic), IL-6 transgenic male mice (Jackson Laboratories) (22), as well as genetic and pharmacologic Fxn knockout models (described below) were subjected to 3 weeks of normobaric hypoxia in a temperature-humidity

controlled chamber (10% O_2, OxyCycler chamber, Biospherix Ltd.) compared with normoxia (21% O_2).

Monocrotaline-treated rats: Lung tissues from male Sprague-Dawley rats (Charles River) at 12 weeks old were injected with 60 mg/kg (i.p.) monocrotaline vs. vehicle control. After 4 weeks, hemodynamic and histologic measurement of pulmonary vascular disease was performed, as we previously described (4).

PH-HFpEF in rats: In a two-hit model of Group 2 PH with metabolic syndrome, double-leptin receptor defect (obese) ZSF1 male rats (Charles River) were treated with a subcutaneous injection of Sugen (SU4516, 100mg/kg, Sigma) at 8-10 weeks-old compared to lean littermate controls. Hemodynamic assessment and tissue procurement were performed 14 weeks after injection (**Supplemental Table 1**) (23).

Inducible cell-specific FXN knockout mice: Fxn *flox/flox* mice (*Fxn* f/f) (24) (from R.M. Payne and H. Puccio) crossed with mice expressing either Cdh5(PAC)-ERT2+-Cre (EC *Fxn*-/-) (25) (from R. Adams) or Myh11-ERT2+-Cre recombinase (SMC *Fxn*-/-) (Jackson Laboratories, Catalog 019079) (26) were administered tamoxifen (2mg/day for five consecutive days) at 10 weeks of age. Two weeks later, mice were placed in normobaric hypoxia in a temperature-humidity controlled chamber (10% O_2, OxyCycler chamber, Biospherix Ltd.) compared with normoxia (21% O_2) for 3 weeks prior to hemodynamic assessment and tissue procurement. For experiments using the senolytic ABT-263, EC *Fxn*-/- mice received drug (25mg/kg/day, based on prior doses used in mice (27, 28)), diluted in DMSO and resuspended in corn oil compared to vehicle control (4% DMSO in corn oil) via daily oral gavage during weeks 2 and 3 of hypoxic exposure.

Generation and delivery of 7C1 nanoparticles containing RNAi

The polymeric nanoparticle 7C1, composed of low molecular weight polyamines and lipids, was utilized for endothelial-specific delivery of FXN siRNA oligonucleotides in C57BL/6 mice (Taconic), as described previously (6, 29, 30). Male mice received tail-vein intravenous doses of FXN siRNA (Stealth siRNA, Life Technologies, 1mg/kg) or scramble control siRNA (Stealth siRNA, Life Technologies, 1mg/kg) formulated in 7C1 with 5-day intervals before and during (day minus 5, day 0, day 5, day 10) the 2 weeks of hypoxic exposure (10% O_2). Right heart catheterization and echocardiography were performed prior to tissue harvest on day 14.

Rodent cardiac and hemodynamic assessments

Echocardiography was performed using a 15-45MHz transthoracic transducer and a VisualSonics Vevo 3100 system (Fujifilm). Inhaled isoflurane anesthesia was used at 2% in 100% O_2 during positioning and hair removal and then decreased to isoflurane 0.8% during imaging. Digital echocardiograms were analyzed off-line for quantitative analysis as previously described (31). Non-invasive tail cuff plethysmography and subsequent closed-chest right heart catheterization were performed, as previously described (31).

Tissue harvest of rodent lungs

After physiological measurements by direct right ventricular puncture, organs were harvested and prepared as previously described (4) and pulmonary vascular endothelial cells were isolated as we previously reported (6). Briefly, mouse lung tissue was digested using Type IV collagenase (2mg/ml, Worthington Biochemical) with agitation via magnetic stir bar in a 37 degree C water bath for 40 minutes. Samples were passed through 40μm Sterile Nylon Mesh Strainers (Fisherbrand), and enzyme activity was terminated with autoMACS Rinsing solution (Miltenyi Biotec). After centrifugation and removal of supernatant, the cell pellets was resuspended in ACK lysis buffer (Thermofisher Scientific) for 3 minutes on ice to remove RBCs. The lysing solution was neutralized with an equal volume of FACS buffer followed by centrifugation and aspiration of the supernatant. Cells were incubated with rat anti-mouse CD31 microbeads and autoMACS Rinsing solution (Miltenyi Biotec) on ice for 15 minutes. Each suspension was filtered through an MS column on a MACS magnetic separator (Miltenyi Biotec) and the column washed with 500μl of autoMACS Rinsing solution three times. Using the plunger, an additional volume of Rinsing solution pushed through the column containing the CD31+ cells which were then prepared for downstream transcript expression analysis.

Immunofluorescent staining and confocal microscopy

Prior work by our laboratory (4, 6, 30-32) and our collaborators (23, 33) have demonstrated that the animal and patient models used exhibit significant pulmonary vascular remodeling. Cryostat sections (5-7μm) from OCT-embedded lung tissues were mounted on gelatin-coated histological slides (Fisherbrand). Following rehydration with PBS for 5 minutes, sections were blocked with 5% donkey serum and 2% BSA in PBS for 1 hour at room temperature. Primary antibodies were diluted in 2% BSA and incubated at 4 degrees C overnight. A complete antibody summary is included in **Supplemental Table 8**. For immunofluorescence, Alexa 488, 568 and 647-conjugated secondary antibodies were purchased from ThermoFisher Scientific. Pictures were obtained using Nikon A1 confocal microscope and 40x oil immersion lens. Small pulmonary vessels (30-100μm diameter) present in a given tissue section (≥10 vessels/section) that were not associated with bronchial airways were selected for analysis. Intensity of staining was quantified using ImageJ software (NIH). Degree of pulmonary arteriolar medial thickening and muscularization were assessed in OCT lung sections stained for α-SMA by calculation of the proportion of fully versus partially muscularized peripheral pulmonary arterioles compared to total peripheral pulmonary arterioles, as previously described (31). Relative medial and adventitial wall thickness was also measured in pulmonary arterioles using ImageJ software (NIH) and expressed as relative fold change, as previously described (31). Analyses were performed blinded to condition.

ELISA

The ELISA kit measuring the level of secreted of secreted interleukin-6 (IL-6) in mouse plasma (Sigma Aldrich) was used according to the manufacturer instructions while colorimetric change was measured by spectrophotometer (Biotek).

Picrosirius red staining and polarized light microscopy

For connective tissue visualization, OCT lung sections from endothelial-specific *Fxn*-/- mice compared to *Fxn*+/+ controls were stained using the Picro Sirius Red Stain kit (Abcam) per the manufacturer's protocol. Imaging of small pulmonary vessels (30-100μm diameter) using parallel and orthogonal light was performed with the Olympus Provis 1 Fluorescent microscope while orthogonal light image intensity (IntDen) was quantified with ImageJ software (NIH) in a blinded fashion and presented as the relative fold change of collagen.

Human samples

PH was defined by elevated mean pulmonary arterial pressure (mPAP) ≥ 25 mmHg. Paraffin-embedded lung samples were collected from discarded surgical samples or rapid autopsy samples from subjects diagnosed with PH (**Supplemental Tables 2-4**) (6, 7) or subjects with FRDA (**Supplemental Table 6**). Non-diseased lung specimens were from the Center for Organ Recovery & Education (CORE), Pittsburgh, PA, USA.

Immunohistochemical staining of lungs from patients with Friedreich's ataxia compared to control

Formalin-fixed and paraffin-embedded lungs were incubated at 37 degrees C for >1h prior to step-wise deparaffinization with Xylene and ethanol (100% → 95% → 70%). Antigen retrieval was performed using BOND Epitope Retrieval Solution 1 (Leica Biosystems) followed by blocking and primary antibody incubation (1:200 CD31, Dako JC70A) overnight at 4 degrees C. Application of biotinylated secondary antibody (Vector Laboratories BA-1300) followed by ABC Detection IHC

Kit (Abcam ab64261) and DAB Substrate Kit (Abcam ab64238) were performed with appropriate washes in between steps. Lungs were then counterstained with hematoxylin for 5 minutes at room temperature. Finally, samples were dehydrated with increasing concentrations of ethyl alcohol and xylene and a coverslip was mounted using Richard-Allen Scientific Cytoseal60 prior to imaging. Lung tissues from patients with Friedreich's ataxia were stained using the above protocol and imaged using Leica Biosystems in the Mayo Clinic Cancer Center Pathology Research Core. Age- and gender-matched control lungs from the University of Pittsburgh Center for Organ Recovery & Education (CORE) were stained using the same protocol and imaged use the Olympus Provis 1 Fluorescent microscope. These samples are summarized in **Supplemental Table 6**. Vessel remodeling of the pulmonary arterioles, including medial and adventitial hypertrophy as well as inflammatory infiltrate, was quantified (average wall thickness/diameter) with ImageJ software (NIH) in a blinded manner. Data was presented as the relative fold change in vessel remodeling with each patient sample representing a weighted average of quantified lung vessels.

Supplemental Tables

Supplemental Table 1. Hemodynamic data for ZSF1 rat model of Group 2 PH-HFpEF (23)

Treatment	***RVSP (mmHg)**
Lean	28
Lean	23
Lean	15
Lean	17
Lean	30
Lean	28
Lean	29
Lean	33
Lean	28
Ob-Su	43
Ob-Su	43
Ob-Su	37
Ob-Su	36
Ob-Su	42
Ob-Su	40
Ob-Su	36
Ob-Su	31
Ob-Su	39

*Right ventricular systolic pressure

Supplemental Table 2. Clinical information for Group 1 PAH patients (6)

Age	Gender	mPAP (mmHg)	Diagnosis	Clinical description
34	Female	50	Idiopathic	Cardiopulmonary arrest (autopsy)
64	Female	55	Idiopathic	Cardiopulmonary arrest (autopsy)
68	Female	44	Scleroderma	Bilateral lung transplant
1	Male	50	Trisomy 21	Lung resection
12	Male	53	BMPR2 Mutation	Bilateral lung transplant
16	Male	62	Idiopathic	Bilateral lung transplant
19	Male	48	Idiopathic	Lung resection
42	Male	57	Scleroderma	Bilateral lung transplant

mPAP, Mean pulmonary arterial pressure

Supplemental Table 3. Clinical information for Group 3 IPF-PH PH patients (6)

Age	**Gender**	**mPAP (mmHg)**	**Diagnosis**	**Clinical description**
69	Female	29	IPF and PH	Bilateral lung transplant
50	Male	30	IPF and PH	Bilateral lung transplant
58	Male	28	IPF and PH	Bilateral lung transplant
61	Male	37	IPF and PH	Bilateral lung transplant
62	Male	28	IPF and PH	Bilateral lung transplant
63	Male	27	IPF and PH	Bilateral lung transplant
66	Male	34	IPF and PH	Bilateral lung transplant
72	Male	46	IPF and PH	Rapid autopsy

Supplemental Table 4. Clinical information for patient lung samples analyzed by single cell RNA sequencing. Clinical characteristics were previously described (7), with matching for age and absence of senescence-altering medications (*i.e.*, oral contraception).

Age	Gender	Diagnosis	Clinical description	Sampled tissue
21	Male	Idiopathic PAH	Bilateral lung transplant	Lung and pulmonary artery
50	Female	Idiopathic PAH	Bilateral lung transplant	Lung
36	Female	Idiopathic PAH	Bilateral lung transplant	Lung
56	Male	Control	Bilateral lung transplant	Lung
55	Male	Control	Bilateral lung transplant	Lung
23	Female	Control	Bilateral lung transplant	Lung
18	Male	Control	Bilateral lung transplant	Lung

Supplemental Table 5. Differential gene expression from RNA sequencing of cultured endothelial cells treated with FXN siRNA compared to control (log2FoldChange > |1.2|, *padj > 0.05).

GeneID	log2FoldChange	*lfcSE	pvalue	*padj
RIBC2	3.569134422	0.400847688	5.39E-19	2.37E-17
SUV39H1	3.226929067	0.684615373	2.44E-06	2.52E-05
RRM2	2.93278685	0.135322023	3.72E-104	3.85E-101
PLK1	2.875692761	0.243103076	2.76E-32	3.05E-30
MCM2	2.803988837	0.237315563	3.25E-32	3.57E-30
MND1	2.748418509	0.256539798	8.80E-27	6.90E-25
MCM10	2.743411594	0.130049527	8.82E-99	6.73E-96
PBK	2.705440546	0.162731197	4.58E-62	1.44E-59
HIST1H2AI	2.69730566	0.214328723	2.56E-36	3.34E-34
FAM111B	2.68469146	0.304521088	1.19E-18	4.97E-17
KIF14	2.674996165	0.193808126	2.47E-43	4.02E-41
CCNA1	2.655432007	0.159229764	1.94E-62	6.23E-60
PKMYT1	2.634660924	0.275849733	1.28E-21	7.00E-20
CLSPN	2.621023469	0.122213049	4.94E-102	4.21E-99
AURKB	2.6049598	0.145116674	4.73E-72	2.14E-69
HMMR	2.575849472	0.2423893	2.23E-26	1.70E-24
EXO1	2.570756578	0.304753541	3.30E-17	1.25E-15
E2F2	2.559136062	0.2884234	7.13E-19	3.08E-17
AC112777.1	2.557590933	0.277690601	3.25E-20	1.60E-18
DEPDC1B	2.549993068	0.226547726	2.17E-29	2.00E-27
AC112198.2	2.549583269	0.413713736	7.15E-10	1.29E-08
ZNF367	2.548969437	0.254526122	1.32E-23	8.25E-22
CDC6	2.537647741	0.162690075	7.51E-55	1.75E-52
E2F8	2.514100594	0.229488744	6.27E-28	5.35E-26
HIST1H3J	2.512567742	0.215161532	1.66E-31	1.74E-29
HIST1H1A	2.507398563	0.187554399	9.19E-41	1.40E-38
CDC20P1	2.491629084	0.260572608	1.15E-21	6.31E-20
HIST1H1B	2.478934387	0.203852361	5.05E-34	6.10E-32
MKI67	2.45326694	0.172962321	1.15E-45	2.04E-43
ZWINT	2.435619918	0.141251497	1.26E-66	4.94E-64
UBE2C	2.430239053	0.122579577	1.78E-87	1.03E-84
SHCBP1	2.428479982	0.089867898	7.98E-161	3.86E-157
CDC20	2.422717273	0.149750423	7.17E-59	2.00E-56
LMNB1	2.419973442	0.170255549	7.53E-46	1.38E-43
E2F1	2.411863468	0.296775279	4.40E-16	1.52E-14

BUB1B	2.404951519	0.118735796	3.23E-91	2.13E-88
HIST1H2BL	2.384675789	0.214363081	9.54E-29	8.48E-27
CDC25C	2.379738654	0.163956524	9.81E-48	1.92E-45
SPC25	2.373687699	0.153066068	3.08E-54	6.87E-52
CENPF	2.372068558	0.195913213	9.61E-34	1.14E-31
HIST2H3D	2.36909182	0.223187505	2.54E-26	1.93E-24
HIST1H1D	2.367605192	0.209999981	1.76E-29	1.63E-27
LOC100505658	2.354041222	0.798168666	0.003184916	0.014699689
ESPL1	2.333527851	0.185444919	2.61E-36	3.37E-34
HIST2H3A	2.326928898	0.19096621	3.74E-34	4.55E-32
HIST2H3C	2.326928898	0.19096621	3.74E-34	4.55E-32
CDC45	2.30452412	0.111402394	4.58E-95	3.32E-92
CDCA2	2.300918068	0.096480377	1.05E-125	1.52E-122
ORC1	2.295665737	0.146010766	1.06E-55	2.60E-53
FBXO43	2.287580956	0.321966591	1.20E-12	3.07E-11
ASPM	2.28456541	0.168372002	6.15E-42	9.80E-40
GAPDHP55	2.282182233	0.792166106	0.003964924	0.01770856
NEK2	2.279906597	0.194957369	1.36E-31	1.44E-29
NCAPG	2.253717777	0.18947267	1.26E-32	1.41E-30
ESCO2	2.252081432	0.287615777	4.87E-15	1.55E-13
PIMREG	2.24965097	0.130179613	6.53E-67	2.63E-64
KIF15	2.249587063	0.188043094	5.54E-33	6.23E-31
CENPE	2.244570255	0.271617388	1.41E-16	5.09E-15
MFSD2A	2.232941161	0.303663457	1.93E-13	5.28E-12
NCAPG2	2.232745025	0.076442734	1.53E-187	2.22E-183
HIST1H2AG	2.217633033	0.215536753	7.91E-25	5.33E-23
CENPM	2.217543584	0.160968539	3.54E-43	5.70E-41
ERCC6L	2.214179955	0.391346468	1.53E-08	2.29E-07
FST	2.197534288	0.183090863	3.45E-33	3.94E-31
CEP55	2.197443918	0.229263762	9.27E-22	5.19E-20
HIST1H3D	2.192605613	0.228325909	7.77E-22	4.36E-20
SPAG5	2.189401636	0.0873912	1.62E-138	2.94E-135
SNORD3B-2	2.188683118	0.340712067	1.33E-10	2.62E-09
TOP2A	2.185275396	0.208689356	1.17E-25	8.64E-24
PSMC3IP	2.180037755	0.196025549	9.89E-29	8.75E-27
NUF2	2.175473196	0.223493796	2.16E-22	1.29E-20
HJURP	2.172582131	0.107625607	1.29E-90	8.11E-88
GTSE1	2.171515245	0.191011794	6.00E-30	5.69E-28
CCND1	2.167255495	0.171292331	1.09E-36	1.46E-34

CDCA8	2.166042451	0.135836069	3.04E-57	7.72E-55
POLQ	2.165160413	0.15240582	8.34E-46	1.51E-43
CCSAP	2.147179649	0.143063117	6.45E-51	1.42E-48
AC016394.1	2.146829451	0.257895704	8.48E-17	3.13E-15
CCNA2	2.144868339	0.079248092	2.53E-161	1.83E-157
DLGAP5	2.144091356	0.243189192	1.18E-18	4.96E-17
TTK	2.141556617	0.271892854	3.37E-15	1.09E-13
TROAP	2.134561195	0.142527683	1.05E-50	2.26E-48
SAPCD2	2.125469841	0.465285725	4.92E-06	4.76E-05
KIF18B	2.125282521	0.244452535	3.50E-18	1.41E-16
NCAPH	2.124126711	0.213189878	2.20E-23	1.37E-21
TRBC2	2.121370833	0.175200614	9.55E-34	1.14E-31
RAD51AP1	2.10566617	0.208678135	6.09E-24	3.90E-22
KIF2C	2.101283936	0.099608006	8.74E-99	6.73E-96
MCM4	2.098748743	0.160453288	4.28E-39	6.20E-37
CDK1	2.097086049	0.216273251	3.12E-22	1.82E-20
SPC24	2.070427734	0.18146983	3.76E-30	3.64E-28
KIF4A	2.070127899	0.112954717	5.03E-75	2.61E-72
CENPU	2.065807556	0.309873216	2.62E-11	5.63E-10
TICRR	2.060711046	0.181769477	8.61E-30	8.10E-28
SLC26A2	2.052786087	0.093894486	5.89E-106	7.11E-103
MYBL2	2.0430817	0.222819035	4.76E-20	2.31E-18
SH2D5	2.040567437	0.330136711	6.37E-10	1.15E-08
TK1	2.037600989	0.188019157	2.29E-27	1.88E-25
PRC1	2.037180554	0.089088847	9.94E-116	1.31E-112
VCL	2.032048674	0.199713374	2.57E-24	1.71E-22
APOBEC3B	2.031809067	0.200749626	4.45E-24	2.90E-22
FANCB	2.03025104	0.21890633	1.78E-20	8.95E-19
BUB1	2.027684504	0.123490266	1.38E-60	4.00E-58
SKA1	2.022150418	0.111769803	3.68E-73	1.78E-70
CENPA	2.018394381	0.117612026	5.16E-66	1.97E-63
ZNF695	2.007080077	0.27924381	6.60E-13	1.73E-11
BLM	2.005132525	0.257269486	6.50E-15	2.05E-13
ATAD5	1.997823769	0.120267204	5.75E-62	1.77E-59
HIST2H4A	1.995383418	0.188566044	3.62E-26	2.72E-24
HIST2H4B	1.995383418	0.188566044	3.62E-26	2.72E-24
BIRC5	1.9832642	0.091905783	2.81E-103	2.72E-100
CDCA5	1.983178292	0.157057157	1.50E-36	1.99E-34
TPX2	1.975850844	0.12376283	2.25E-57	5.82E-55

TYMS	1.972073853	0.111893409	1.60E-69	6.80E-67
RAD54L	1.971130072	0.290702338	1.20E-11	2.67E-10
ARHGAP11A	1.967961615	0.152197734	3.04E-38	4.27E-36
TCF19	1.96769542	0.158141409	1.53E-35	1.95E-33
HIST2H2AA4	1.96521137	0.207899434	3.30E-21	1.73E-19
KNL1	1.962987281	0.190484471	6.67E-25	4.54E-23
HIST1H2BJ	1.961684374	0.188966454	3.02E-25	2.16E-23
ANLN	1.96122788	0.19548341	1.09E-23	6.96E-22
CKAP2L	1.952740864	0.222780786	1.86E-18	7.72E-17
NDUFS1	1.941843152	0.072230538	3.38E-159	1.23E-155
KIF11	1.935206946	0.138010181	1.14E-44	1.97E-42
AC009533.1	1.931136329	0.297001628	7.92E-11	1.61E-09
GINS2	1.929025238	0.098704566	4.69E-85	2.52E-82
U1	1.924579639	0.285444487	1.56E-11	3.43E-10
DHFRP1	1.916018058	0.175454196	9.22E-28	7.72E-26
ATAD2	1.910718204	0.198782643	7.11E-22	4.01E-20
AURKA	1.910217944	0.078096392	3.96E-132	6.38E-129
KIF18A	1.906901454	0.334774283	1.23E-08	1.86E-07
CCNB1	1.896521268	0.112442798	7.93E-64	2.67E-61
DMC1	1.893908916	0.317078726	2.33E-09	3.94E-08
CDCA3	1.893725992	0.157252712	2.12E-33	2.46E-31
DEPDC1	1.893061776	0.22360531	2.54E-17	9.68E-16
GINS1	1.891110811	0.071824285	8.77E-153	2.54E-149
CENPW	1.891032662	0.181410201	1.93E-25	1.40E-23
HMOX1	1.88979321	0.190730623	3.84E-23	2.37E-21
PTTG1	1.885430478	0.162134002	2.94E-31	3.05E-29
RTKN2	1.877431788	0.247551639	3.35E-14	1.01E-12
HIST2H2BF	1.873433958	0.118232718	1.51E-56	3.79E-54
HIST2H2BB	1.872271499	0.253235671	1.43E-13	3.95E-12
FEN1	1.869096579	0.085523835	7.02E-106	7.82E-103
CCNB2	1.86781101	0.113607078	9.73E-61	2.88E-58
MCM7	1.862612514	0.162300684	1.74E-30	1.72E-28
NUSAP1	1.857066384	0.230980076	8.99E-16	3.03E-14
CKS1B	1.84910032	0.201710657	4.86E-20	2.34E-18
NDC80	1.845181819	0.194088826	1.96E-21	1.05E-19
ASF1B	1.841096821	0.194281086	2.63E-21	1.40E-19
SKA3	1.831288296	0.273201825	2.04E-11	4.42E-10
RN7SL411P	1.825204802	0.625574962	0.003526872	0.016032945
PCLAF	1.818238668	0.188422797	4.93E-22	2.82E-20

SGO1	1.815518439	0.155237394	1.35E-31	1.44E-29
POLE2	1.809180142	0.218228196	1.13E-16	4.10E-15
KIF20B	1.804635151	0.220356113	2.62E-16	9.18E-15
CPA3	1.803660824	0.220393236	2.75E-16	9.58E-15
KSR2	1.791187903	0.337688806	1.13E-07	1.47E-06
PLK4	1.788755834	0.25544433	2.51E-12	6.16E-11
IQGAP3	1.780899961	0.276046795	1.11E-10	2.20E-09
AUNIP	1.772130172	0.200825119	1.10E-18	4.66E-17
SCN10A	1.76903547	0.334357352	1.22E-07	1.57E-06
MTFR2	1.766605077	0.154553644	2.95E-30	2.87E-28
RNU2-63P	1.765862412	0.370508166	1.88E-06	1.99E-05
CIP2A	1.765408631	0.170801361	4.84E-25	3.37E-23
TRAIP	1.763669423	0.187111514	4.27E-21	2.21E-19
KIF20A	1.758355786	0.103535802	1.10E-64	3.97E-62
MAD2L1	1.753616184	0.298168655	4.07E-09	6.59E-08
FBXO5	1.753416649	0.175879754	2.07E-23	1.30E-21
ORC6	1.750242541	0.159215528	4.13E-28	3.57E-26
OIP5	1.746750427	0.193562662	1.81E-19	8.25E-18
HIST1H4H	1.746332521	0.245268636	1.08E-12	2.77E-11
FANCD2	1.739478041	0.099610832	2.75E-68	1.14E-65
BRCA1	1.727748408	0.246151504	2.23E-12	5.51E-11
DIAPH3	1.719223135	0.065901466	5.02E-150	1.21E-146
HPDL	1.716726485	0.418351194	4.07E-05	0.000321951
HELLS	1.714486027	0.184954393	1.87E-20	9.32E-19
MEX3A	1.699883818	0.240704278	1.64E-12	4.14E-11
KIF23	1.697711737	0.151539018	3.94E-29	3.57E-27
CDKN3	1.694736443	0.238392755	1.17E-12	2.99E-11
DDX12P	1.690357233	0.246401941	6.88E-12	1.58E-10
KIF22	1.686732846	0.170370628	4.15E-23	2.55E-21
RACGAP1	1.686475252	0.093919371	4.26E-72	1.99E-69
UBE2T	1.669031519	0.222710071	6.67E-14	1.94E-12
PSKH1	1.66610044	0.256319254	8.03E-11	1.63E-09
BRIP1	1.663633058	0.190727795	2.72E-18	1.11E-16
FOXM1	1.657876762	0.186557726	6.30E-19	2.75E-17
RFC3	1.656086929	0.226793673	2.83E-13	7.62E-12
CENPN	1.653951254	0.143747117	1.23E-30	1.24E-28
HIST1H1C	1.653230961	0.140871276	8.36E-32	8.97E-30
ERBB4	1.64879566	0.36137769	5.05E-06	4.88E-05
AMMECR1	1.64750642	0.117661569	1.51E-44	2.58E-42

HIST1H2AD	1.629814817	0.248935132	5.86E-11	1.21E-09
CDT1	1.624616336	0.271777264	2.26E-09	3.83E-08
ELOA	1.619931888	0.096030369	7.61E-64	2.63E-61
SGO2	1.618376613	0.264473525	9.40E-10	1.65E-08
FANCI	1.611617021	0.170365559	3.09E-21	1.63E-19
KIF24	1.611142944	0.155031424	2.69E-25	1.93E-23
MCM5	1.610272601	0.224447781	7.26E-13	1.89E-11
MELK	1.599830917	0.099917313	1.06E-57	2.80E-55
ESM1	1.598155711	0.121904734	2.89E-39	4.23E-37
HIST2H2AB	1.593343061	0.222477994	7.96E-13	2.07E-11
HMGB3	1.593084779	0.13760763	5.39E-31	5.50E-29
CENPI	1.592636565	0.176098859	1.51E-19	6.97E-18
AC025186.1	1.589836916	0.58660983	0.006724024	0.027606395
EZH2	1.587865025	0.107350506	1.66E-49	3.45E-47
PSRC1	1.568642191	0.146373335	8.50E-27	6.69E-25
HMGB2	1.568040553	0.155933205	8.66E-24	5.53E-22
TRIP13	1.565748672	0.093384208	4.27E-63	1.41E-60
ZGRF1	1.560556364	0.312504321	5.92E-07	6.83E-06
EME1	1.545264262	0.194783879	2.14E-15	7.04E-14
CDCA7	1.544947061	0.16155121	1.14E-21	6.29E-20
DNAJC9	1.54045667	0.144617459	1.71E-26	1.32E-24
BRI3BP	1.539131333	0.128223623	3.41E-33	3.92E-31
CDC25A	1.528392527	0.204362954	7.50E-14	2.16E-12
NCR3LG1	1.526528918	0.148114356	6.59E-25	4.51E-23
AC099850.3	1.526193909	0.206950054	1.65E-13	4.51E-12
PCNA	1.526114909	0.12738515	4.51E-33	5.10E-31
POC1A	1.523358479	0.155738347	1.35E-22	8.23E-21
H2AFX	1.518253001	0.216474545	2.32E-12	5.70E-11
PMCH	1.514486083	0.313315286	1.34E-06	1.45E-05
XRCC2	1.512620554	0.184551166	2.48E-16	8.71E-15
PRC1-AS1	1.511133029	0.294910812	2.99E-07	3.63E-06
PRR11	1.511015786	0.155517755	2.58E-22	1.52E-20
CHAF1A	1.509722452	0.202934206	1.01E-13	2.85E-12
MT1L	1.508905864	0.176538558	1.26E-17	4.89E-16
DSCC1	1.504964796	0.20130435	7.66E-14	2.19E-12
CENPH	1.499182622	0.193875762	1.05E-14	3.26E-13
HIST1H4C	1.496480525	0.266210085	1.89E-08	2.77E-07
ITPRIPL1	1.495747648	0.417157243	0.000336339	0.00211006
WDR76	1.492004765	0.180065386	1.17E-16	4.25E-15

RECQL4	1.481551566	0.39916842	0.000205957	0.001370873
ATXN7L3B	1.478658665	0.073604386	9.16E-90	5.53E-87
PRIM1	1.476483709	0.233865582	2.73E-10	5.21E-09
FRMD3	1.474895613	0.145407627	3.55E-24	2.34E-22
TMPPE	1.463599399	0.178808102	2.72E-16	9.49E-15
LOC101928000	1.463464179	0.361736369	5.22E-05	0.000400836
DHFR	1.455652558	0.155771193	9.21E-21	4.70E-19
WDR62	1.45562888	0.144182152	5.77E-24	3.72E-22
MTBP	1.450294584	0.229874112	2.81E-10	5.35E-09
MCM6	1.448839803	0.110166246	1.67E-39	2.47E-37
GINS3	1.448665964	0.092316649	1.71E-55	4.12E-53
RNU5A-8P	1.441365996	0.554439365	0.00933102	0.0361496
AC124798.1	1.43547415	0.288920294	6.75E-07	7.72E-06
AC025257.1	1.435323873	0.42306591	0.000692145	0.003951958
NEIL3	1.42613477	0.171804742	1.03E-16	3.78E-15
CORO1A	1.422687989	0.322336818	1.02E-05	9.17E-05
C17orf53	1.417045651	0.206585541	6.92E-12	1.58E-10
RRM1	1.415645322	0.12924335	6.40E-28	5.43E-26
HIST1H2BK	1.414069006	0.135892129	2.33E-25	1.68E-23
DKC1	1.412619666	0.085620584	3.76E-61	1.13E-58
DNA2	1.411034139	0.250216147	1.71E-08	2.53E-07
H2AFZ	1.410132108	0.161245476	2.23E-18	9.14E-17
POLR3G	1.408553799	0.268686844	1.59E-07	2.01E-06
STIL	1.408315062	0.188614837	8.23E-14	2.34E-12
CIT	1.402590634	0.148206207	2.97E-21	1.57E-19
ANKRD18B	1.401137311	0.20301662	5.14E-12	1.20E-10
LMNB2	1.400383081	0.258070796	5.75E-08	7.79E-07
CAAP1	1.398951442	0.110878439	1.70E-36	2.24E-34
DTL	1.392999398	0.134405619	3.61E-25	2.53E-23
CEP128	1.392216033	0.156457814	5.67E-19	2.49E-17
AC129102.1	1.388891685	0.224253674	5.89E-10	1.07E-08
SASS6	1.388453037	0.251878145	3.54E-08	4.98E-07
CCDC190	1.378607546	0.332483923	3.38E-05	0.000272786
TEDC2	1.375736918	0.278699819	7.96E-07	9.00E-06
RMI2	1.369175441	0.166508505	1.99E-16	7.04E-15
RNU5D-1	1.367146431	0.459628059	0.002935023	0.013729923
CENPK	1.366143922	0.215515497	2.31E-10	4.44E-09
CDKN2C	1.363052746	0.252010537	6.35E-08	8.54E-07
CCDC150	1.359950427	0.176186171	1.17E-14	3.61E-13

MMS22L	1.35992528	0.241207605	1.72E-08	2.54E-07
RAD51	1.358335984	0.141955065	1.08E-21	6.01E-20
MYBL1	1.350848346	0.195855932	5.31E-12	1.23E-10
SKINT1L	1.349785709	0.474444638	0.004441415	0.019505361
MAT2B	1.348570166	0.121099711	8.38E-29	7.50E-27
AC012073.1	1.348303005	0.272026006	7.18E-07	8.19E-06
TACC3	1.344151684	0.242672758	3.04E-08	4.33E-07
SMC2	1.33804234	0.235346362	1.30E-08	1.97E-07
EPS15	1.336006531	0.151483771	1.15E-18	4.85E-17
SNRPD1	1.332255115	0.154393518	6.19E-18	2.46E-16
HASPIN	1.331510418	0.277157104	1.55E-06	1.67E-05
PARPBP	1.330128058	0.265565716	5.48E-07	6.37E-06
NCAPD3	1.328894028	0.149199523	5.25E-19	2.32E-17
FAM217B	1.323541842	0.196035733	1.46E-11	3.24E-10
NPIPB13	1.322955488	0.478832621	0.005729441	0.024138245
AC093724.1	1.321790257	0.199241349	3.26E-11	6.96E-10
INCENP	1.320502427	0.29495413	7.57E-06	7.02E-05
HDAC9	1.318398361	0.186896776	1.74E-12	4.37E-11
DPF1	1.31004718	0.221058133	3.10E-09	5.11E-08
UBE2L2	1.307386758	0.49619484	0.008418058	0.03331602
MCM8	1.306006611	0.187600372	3.36E-12	8.10E-11
COPZ1	1.304481998	0.11875968	4.55E-28	3.90E-26
KIF21A	1.301018403	0.187879412	4.37E-12	1.04E-10
ARHGAP11B	1.296531029	0.229194736	1.54E-08	2.30E-07
LOC100288637	1.296531029	0.229194736	1.54E-08	2.30E-07
HK2	1.293134263	0.319043804	5.05E-05	0.000389241
HIST1H2BD	1.292667751	0.174725612	1.38E-13	3.82E-12
CCNE2	1.290631503	0.253816866	3.68E-07	4.40E-06
BRCA2	1.287333456	0.25720159	5.58E-07	6.47E-06
SNAPIN	1.28388851	0.139074699	2.67E-20	1.32E-18
KNSTRN	1.283829918	0.152069144	3.11E-17	1.18E-15
PANK3	1.283706085	0.124384668	5.70E-25	3.93E-23
C1orf112	1.277229114	0.208628105	9.24E-10	1.63E-08
AC007952.4	1.27694874	0.173789164	2.02E-13	5.50E-12
HIST2H2BE	1.276167311	0.111071748	1.49E-30	1.49E-28
SPINT1	1.275970425	0.410646329	0.001888528	0.009440685
NUP43	1.273228155	0.087653408	8.33E-48	1.65E-45
CCNF	1.266696247	0.225809375	2.03E-08	2.96E-07
RNVU1-15	1.264210997	0.358926052	0.000427974	0.002604674

FANCA	1.260435183	0.14176809	6.07E-19	2.66E-17
WDHD1	1.259835604	0.202412651	4.84E-10	8.91E-09
AC092718.4	1.258282344	0.172091186	2.64E-13	7.12E-12
EMC8	1.251031503	0.12813652	1.62E-22	9.82E-21
AC004837.3	1.247782254	0.192188693	8.44E-11	1.71E-09
GINS4	1.242146216	0.256511517	1.28E-06	1.40E-05
PDE4A	1.239440025	0.227566561	5.14E-08	7.00E-07
HIST1H1E	1.235739421	0.136006107	1.03E-19	4.81E-18
PAQR4	1.235049262	0.348902824	0.000400417	0.002458639
CCDC34	1.234596999	0.196854914	3.57E-10	6.75E-09
AP005901.5	1.227887421	0.478770777	0.010327499	0.039306313
HIST1H2BN	1.226429625	0.136435117	2.49E-19	1.12E-17
RFC4	1.22200686	0.164667388	1.16E-13	3.25E-12
CEP72	1.215965959	0.277614325	1.19E-05	0.000105713
AC016205.1	1.21231496	0.399766853	0.002424929	0.011648177
CENPL	1.210675566	0.159028359	2.68E-14	8.07E-13
INHBA	1.207369506	0.131671659	4.75E-20	2.31E-18
AL359955.1	1.207003409	0.372386219	0.001189994	0.00629611
TGFBR2	-1.201063689	0.135835142	9.40E-19	3.99E-17
BAALC	-1.204504116	0.240663039	5.59E-07	6.48E-06
PDGFRA	-1.204727365	0.258212477	3.08E-06	3.12E-05
ZNF366	-1.206200258	0.153673723	4.19E-15	1.34E-13
GADD45A	-1.207406483	0.134802447	3.34E-19	1.49E-17
UST	-1.210405836	0.35446632	0.000638459	0.003678751
AC046143.1	-1.210724048	0.229916555	1.39E-07	1.79E-06
FAM129A	-1.217603711	0.191924166	2.24E-10	4.30E-09
NOTCH4	-1.219238441	0.390520279	0.001795736	0.009017246
KAT2B	-1.225794323	0.149385668	2.30E-16	8.10E-15
CLU	-1.226028833	0.279337958	1.14E-05	0.000101856
COL1A2	-1.233110106	0.249780009	7.94E-07	8.99E-06
P4HA3	-1.233504589	0.127066118	2.80E-22	1.64E-20
TCTEX1D1	-1.234669381	0.156406352	2.93E-15	9.51E-14
ADIRF	-1.235885215	0.11346566	1.26E-27	1.03E-25
LYNX1	-1.237324861	0.435568524	0.00450129	0.019738416
AL162591.2	-1.239596279	0.186100887	2.72E-11	5.85E-10
SCG5	-1.240790136	0.347984005	0.000362952	0.002251481
LIMCH1	-1.241228008	0.07713306	2.90E-58	7.94E-56
PCDHB14	-1.246577463	0.28439491	1.17E-05	0.000104239
RAET1E	-1.250679218	0.274005252	5.01E-06	4.84E-05

LAYN	-1.251019562	0.243032076	2.64E-07	3.23E-06
C5orf24	-1.251849991	0.100967396	2.66E-35	3.35E-33
LRRC17	-1.256482265	0.244769721	2.85E-07	3.46E-06
A2M	-1.264572276	0.238543709	1.15E-07	1.49E-06
ARRDC2	-1.267367564	0.233532156	5.73E-08	7.77E-07
HTR1D	-1.274253533	0.277220381	4.30E-06	4.21E-05
GPR153	-1.274446617	0.41049347	0.001904917	0.009512771
ECM1	-1.27838442	0.329460088	0.000104353	0.000740121
ERV3-1-ZNF117	-1.283426189	0.253953209	4.33E-07	5.10E-06
ZNF117	-1.283426189	0.253953209	4.33E-07	5.10E-06
ST6GALNAC3	-1.285673243	0.208835538	7.44E-10	1.34E-08
TFPI	-1.286311191	0.185821007	4.44E-12	1.05E-10
COMMD8	-1.290753736	0.199643316	1.01E-10	2.03E-09
SULT1A4	-1.291052888	0.470999473	0.006123536	0.025509454
RAET1G	-1.292043371	0.372738327	0.000527566	0.003122959
CTNNBIP1	-1.292256361	0.178297762	4.24E-13	1.13E-11
LRRC4	-1.292639173	0.327849098	8.05E-05	0.000590289
ERMAP	-1.297277846	0.10530606	7.15E-35	8.93E-33
DKK3	-1.300223282	0.177150162	2.14E-13	5.80E-12
C16orf45	-1.303789826	0.096728776	2.08E-41	3.25E-39
AL359075.2	-1.308667027	0.246944568	1.16E-07	1.51E-06
FABP5P7	-1.317383831	0.199044708	3.63E-11	7.68E-10
LZTS3	-1.319350695	0.438681437	0.00263374	0.012497979
MRC2	-1.32361	0.309662293	1.92E-05	0.000163363
VWCE	-1.327737587	0.234533057	1.50E-08	2.26E-07
TGFBI	-1.33110736	0.231365566	8.75E-09	1.36E-07
CACNA2D4	-1.33212132	0.289171691	4.09E-06	4.03E-05
SLFN5	-1.333378369	0.101171992	1.15E-39	1.73E-37
DPP4	-1.336267281	0.083225901	5.20E-58	1.40E-55
CLDN10	-1.339695961	0.286426589	2.91E-06	2.96E-05
CD302	-1.34165915	0.157614151	1.71E-17	6.56E-16
UNC5A	-1.342312134	0.313888695	1.90E-05	0.000161977
TNFRSF10C	-1.343264628	0.191322803	2.20E-12	5.45E-11
OLFML3	-1.344992827	0.149156134	1.93E-19	8.76E-18
NIPAL2	-1.348545197	0.21734338	5.48E-10	1.00E-08
MAN2A1	-1.349793534	0.103820153	1.20E-38	1.73E-36
TNFRSF4	-1.353258871	0.36659772	0.000223023	0.001470957
GALNT15	-1.360911938	0.100759367	1.43E-41	2.25E-39

ANGPTL4	-1.3631653	0.293890141	3.51E-06	3.50E-05
VSIR	-1.364493736	0.329287851	3.42E-05	0.000275766
VAV3	-1.367763011	0.208451746	5.33E-11	1.10E-09
CTSO	-1.370401505	0.12391916	1.99E-28	1.73E-26
CREG2	-1.373646934	0.163188218	3.84E-17	1.45E-15
TMEM273	-1.38454	0.215918706	1.43E-10	2.82E-09
HDHD2	-1.391232217	0.144392866	5.69E-22	3.23E-20
DDR1	-1.395929448	0.473415341	0.003191798	0.014714874
SEPTIN4	-1.399458563	0.234808158	2.52E-09	4.23E-08
FABP5	-1.408454587	0.109457355	6.85E-38	9.37E-36
PCDH12	-1.40937066	0.230046097	8.98E-10	1.59E-08
PKHD1L1	-1.416110326	0.250733227	1.62E-08	2.41E-07
WASF3	-1.424469548	0.163380007	2.81E-18	1.14E-16
C3AR1	-1.42450288	0.314924851	6.09E-06	5.78E-05
NR1H3	-1.437999209	0.137332304	1.17E-25	8.64E-24
MRAP2	-1.447566236	0.153288035	3.61E-21	1.89E-19
ITGA1	-1.449989601	0.194170178	8.17E-14	2.33E-12
ANGPTL2	-1.453009958	0.245042293	3.04E-09	5.02E-08
TSPAN7	-1.461962488	0.259328248	1.73E-08	2.54E-07
GBP1P1	-1.46198008	0.336101096	1.36E-05	0.000119059
PDE1A	-1.464651647	0.500829387	0.00345063	0.015730748
LINC01676	-1.472476651	0.491663416	0.00274546	0.012951818
ANK2	-1.472971609	0.273327918	7.08E-08	9.47E-07
GJA4	-1.479241009	0.211872924	2.92E-12	7.09E-11
CCDC85A	-1.485488714	0.242046871	8.40E-10	1.49E-08
NT5E	-1.487471422	0.08779254	2.17E-64	7.66E-62
RCSD1	-1.494365563	0.214273173	3.08E-12	7.46E-11
C7orf61	-1.494857446	0.167136554	3.76E-19	1.67E-17
PPP1R3C	-1.500423247	0.223125113	1.76E-11	3.86E-10
CASP12	-1.502340871	0.228495517	4.87E-11	1.02E-09
NPR1	-1.513189899	0.20824066	3.69E-13	9.86E-12
STK38L	-1.521639063	0.210955455	5.47E-13	1.44E-11
KLF3-AS1	-1.531333521	0.22152124	4.75E-12	1.12E-10
FKBP9	-1.540300878	0.245471878	3.50E-10	6.63E-09
CASP7	-1.555491842	0.109576061	9.76E-46	1.75E-43
SCN9A	-1.566055956	0.215396683	3.58E-13	9.59E-12
SELE	-1.569000578	0.146951144	1.30E-26	1.02E-24
GIMAP5	-1.571824555	0.088075231	3.08E-71	1.35E-68
STAT4	-1.581922948	0.398309872	7.14E-05	0.000528607

NOD2	-1.59323019	0.428366533	0.000199764	0.001333321
DIRAS3	-1.595976249	0.164393442	2.78E-22	1.64E-20
FLT4	-1.596372751	0.245892619	8.46E-11	1.71E-09
AFAP1L2	-1.598931167	0.165432817	4.24E-22	2.44E-20
CRACR2B	-1.60070439	0.208876832	1.81E-14	5.52E-13
GPER1	-1.601020752	0.330684104	1.29E-06	1.40E-05
ENPP2	-1.601802395	0.357082509	7.26E-06	6.76E-05
CAPN11	-1.606357347	0.344102819	3.04E-06	3.08E-05
TSPAN11	-1.613577268	0.258081897	4.05E-10	7.59E-09
ADAM19	-1.615213679	0.211177472	2.03E-14	6.16E-13
APOL3	-1.629875908	0.089531839	4.76E-74	2.38E-71
STS	-1.639048235	0.12668918	2.76E-38	3.93E-36
MAMDC2	-1.642942096	0.418035652	8.49E-05	0.000617512
CROT	-1.664783399	0.146097094	4.43E-30	4.25E-28
IL17D	-1.66600686	0.280770564	2.96E-09	4.91E-08
C11orf96	-1.666152227	0.248035674	1.85E-11	4.04E-10
GPR143	-1.668640683	0.206570149	6.59E-16	2.24E-14
SLC46A3	-1.670558374	0.120248601	7.03E-44	1.19E-41
DLL4	-1.672419411	0.168010584	2.42E-23	1.50E-21
PRDM8	-1.676699531	0.329053144	3.48E-07	4.17E-06
SELP	-1.677875242	0.43475381	0.00011368	0.000798461
PDE6G	-1.677884802	0.40648409	3.66E-05	0.000293507
ACOX2	-1.684081238	0.269150833	3.92E-10	7.37E-09
PIK3IP1	-1.687564552	0.130772087	4.24E-38	5.85E-36
AC073957.2	-1.689300448	0.162847884	3.27E-25	2.31E-23
AXL	-1.690147602	0.240856099	2.26E-12	5.57E-11
GPR146	-1.692432063	0.457544364	0.000216496	0.001433781
UBE2V2	-1.69897173	0.198770175	1.26E-17	4.89E-16
FER1L6	-1.703367572	0.19243015	8.61E-19	3.67E-17
LOC643733	-1.707144071	0.115239393	1.19E-49	2.54E-47
AC011462.1	-1.733490512	0.395779883	1.19E-05	0.000105713
SLCO2A1	-1.74164529	0.477124966	0.000261943	0.001692239
CSF3	-1.758957931	0.350447914	5.19E-07	6.04E-06
SLC16A6	-1.805787395	0.216814348	8.17E-17	3.03E-15
MAN2B2	-1.824615948	0.282865847	1.12E-10	2.21E-09
FLVCR2	-1.826378202	0.206295951	8.50E-19	3.64E-17
CXCL11	-1.837373834	0.125501707	1.56E-48	3.13E-46
RARRES1	-1.851800234	0.194366375	1.61E-21	8.73E-20
CADM3	-1.87950193	0.37104409	4.07E-07	4.83E-06

CETP	-1.886917403	0.215337645	1.91E-18	7.88E-17
CDA	-1.895993165	0.289693167	5.96E-11	1.22E-09
EFCC1	-1.916545005	0.302492423	2.36E-10	4.53E-09
COL3A1	-1.922798034	0.400769821	1.60E-06	1.72E-05
PDE2A	-1.923922854	0.209271347	3.80E-20	1.87E-18
HTRA3	-1.936347208	0.299806284	1.06E-10	2.10E-09
AC104211.1	-1.937970507	0.340613238	1.27E-08	1.92E-07
ABCG2	-1.944187952	0.124988502	1.47E-54	3.39E-52
DPH6-AS1	-1.951397289	0.371096272	1.45E-07	1.85E-06
C6orf120	-1.986479752	0.097862958	1.32E-91	9.14E-89
CYBRD1	-1.990120579	0.09277984	4.57E-102	4.14E-99
B3GNT9	-1.990880579	0.328600805	1.37E-09	2.38E-08
CX3CL1	-2.001551956	0.275684489	3.86E-13	1.03E-11
AC007744.1	-2.046991166	0.365027613	2.05E-08	2.98E-07
ATE1-AS1	-2.054612175	0.351513597	5.06E-09	8.12E-08
RHOU	-2.055930413	0.421508169	1.07E-06	1.19E-05
TXLNB	-2.123405715	0.274660306	1.07E-14	3.30E-13
HCRTR1	-2.13529697	0.302816325	1.77E-12	4.45E-11
PDK4	-2.233637083	0.087233757	1.34E-144	2.77E-141
CLEC10A	-2.247771733	0.384410875	5.00E-09	8.02E-08
SERPINB2	-2.264074712	0.851791218	0.007860215	0.031432276
INHBB	-2.285054054	0.140815788	3.24E-59	9.20E-57
TMOD1	-2.303103918	0.333270034	4.83E-12	1.13E-10
IFIT2	-2.333650107	0.182553104	2.03E-37	2.75E-35
FXN	-2.344964395	0.15031999	7.30E-55	1.73E-52
MMP28	-2.502987493	0.560054302	7.85E-06	7.23E-05
GALNT1	-2.519354332	0.178350949	2.63E-45	4.60E-43
ABCA1	-2.570443708	0.165412361	1.87E-54	4.24E-52
IDO1	-2.652000567	0.184928747	1.22E-46	2.27E-44
IL33	-2.761173874	0.252976758	9.80E-28	8.17E-26
AQP1	-2.787729624	0.246844638	1.41E-29	1.32E-27
CXCL10	-2.913522824	0.251811246	5.83E-31	5.91E-29
AL731556.1	-3.440277005	0.994222026	0.000539633	0.003178815
INTS6P1	-4.236036704	1.467934863	0.003905298	0.017511632
UBD	-5.303267085	1.344079128	7.96E-05	0.000583867

*lfcSE – Standard error of log2FoldChange, padj – False Discovery Rate adjusted p-value

Supplemental Table 6. Clinical information for patients with Friedreich's ataxia compared to age- and gender-matched controls

*Age (years)	Sex	Patient	*FRDA symptoms	Cardiac findings
41	Male	FRDA 1	Ataxia, pes cavus	Hypertrophic cardiomyopathy (*EF 10%), Refractory atrial tachycardia
43	Male	Control 1A	-	-
37	Male	Control 1B	-	-
44	Male	Control 1C	-	-
20	Male	FRDA 2	Scoliosis, nystagmus, ataxic dysarthria	Dilated cardiomyopathy (*EF 10%), Atrial flutter
25	Male	Control 2A	-	-
13	Male	Control 2B	-	-
26	Male	Control 2C	-	-
63	Female	FRDA 3	Ataxia, dysarthria, hearing loss	Cardiomyopathy (*EF 15%)
66	Female	Control 3A	-	-
68	Female	Control 3B	-	-
66	Male	Control 3C	-	-

*Age – Age of tissue procurement, FRDA – Friedreich's ataxia, EF – Ejection fraction

Supplemental Table 7. Taqman primers

Taqman Primers	Species	Assay ID
ACTB	Human	Hs99999903_m1
	Rat	Rn00667869_m1
	Mouse	Mm02619580_g1
BRD2	Human	Hs01121986_m1
BRD4	Human	Hs04188087_m1
CDH5	Human	Hs00901465_m1
CDKN2A	Human	Hs00923894_m1
	Rat	Rn00580664_m1
	Mouse	Mm00494449_m1
CST3	Mouse	Mm00438347_m1
CTCF	Human	Hs00902016_m1
EDN1	Human	Hs01574659_m1
EPAS1	Human	Hs01026149_m1
FXN	Human	Hs00175940_m1
	Rat	Rn01501403_m1
	Mouse	Mm00784016_m1
GOT1	Mouse	Mm00805379_g1
GPT	Mouse	Mm00435217_m1
HIF1A	Human	Hs00153153_m1
IL1B	Human	Hs01555410_m1
IL6	Human	Hs00174131_m1
ISCU	Human	Hs00384510_m1
LCN2	Mouse	Mm01324470_m1
NOS3	Human	Hs01574659_m1
PECAM1	Human	Hs01065279_m1
SIN3A	Human	Hs00411592_m1
	Rat	Rn01417686_m1
	Mouse	Mm00488255_m1
TNFA	Mouse	Mm00443258_m1

Supplemental Table 8. Antibodies

Antibody	Company	Cat. No.	Species	Concentration
Immunoblot				
ATM	Cell Signaling Technologies	2873T	Rabbit	1 / 1000
p-ATM (Ser1981)	Abcam	ab81292	Rabbit	1 / 1000
ATR	Cell Signaling Technologies	2790S	Rabbit	1 / 1000
p-ATR (Ser428)	Cell Signaling Technologies	2853T	Rabbit	1 / 1000
β-actin	Santa Cruz Biotechnologies	sc47778	Mouse	1 / 1000
BRD2	Abcam	ab139690	Rabbit	1 / 1000
BRD4	Abcam	ab128874	Rabbit	1 / 1000
CHK1	Cell Signaling Technologies	2360S	Mouse	1 / 1000
p-CHK1 (Ser345)	Cell Signaling Technologies	2341T	Rabbit	1 / 1000
CHK2	Cell Signaling Technologies	2662T	Rabbit	1 / 1000
p-CHK2 (Thr68)	Cell Signaling Technologies	2661T	Rabbit	1 / 1000
CTCF	Abcam	ab70303	Rabbit	1 / 1000
FXN	Abcam	ab110328	Mouse	1 / 200
p-γH2AX (Ser139)	Abcam	ab11174	Rabbit	1 / 500
MCM2	Cell Signaling Technologies	3619T	Rabbit	1 / 1000
NOS3	Santa Cruz Biotechnologies	sc376751	Mouse	1 / 1000
CDKN2A/p16INKA	Abcam	ab108349	Rabbit	1 / 1000
p21Cip1	Abcam		Rabbit	1 / 1000
p53	Cell Signaling Technologies	9282T	Rabbit	1 / 500
RPA32	Cell Signaling Technologies	2208T	Rat	1 / 1000
p-RPA32 (Ser4/Ser8)	Bethyl Laboratories	A300-245A-M	Rabbit	1 / 500
RPA70/RPA1	Cell Signaling Technologies	2267S	Rabbit	1 / 1000
Immunofluorescent staining				
CD11b	Abcam	ab197702	Rat	1/100
CD31	Santa Cruz	sc376764	Mouse	1/100
CD144	Abcam	ab33168	Rabbit	1 / 100
BrdU	BD Biosciences	347580	Mouse	1 / 50.
BrdU	Abcam	ab6326	Rat	1 / 75.
FXN	Abcam	ab113691	Mouse	1 / 100
CDKN2A/p16INKA	Abcam	ab108349	Rabbit	1 / 100
a-SMA	Abcam	ab21027	Goat	1 / 350
vWF	Abcam	ab8822	Goat	1 / 50.
Proximity ligation assay				
POLD1	Santa Cruz Biotechnologies	sc-17776	Mouse	1 / 250
POLD3	Bethyl Laboratories	A301-243A	Rabbit	1 / 250

Supplemental Figures

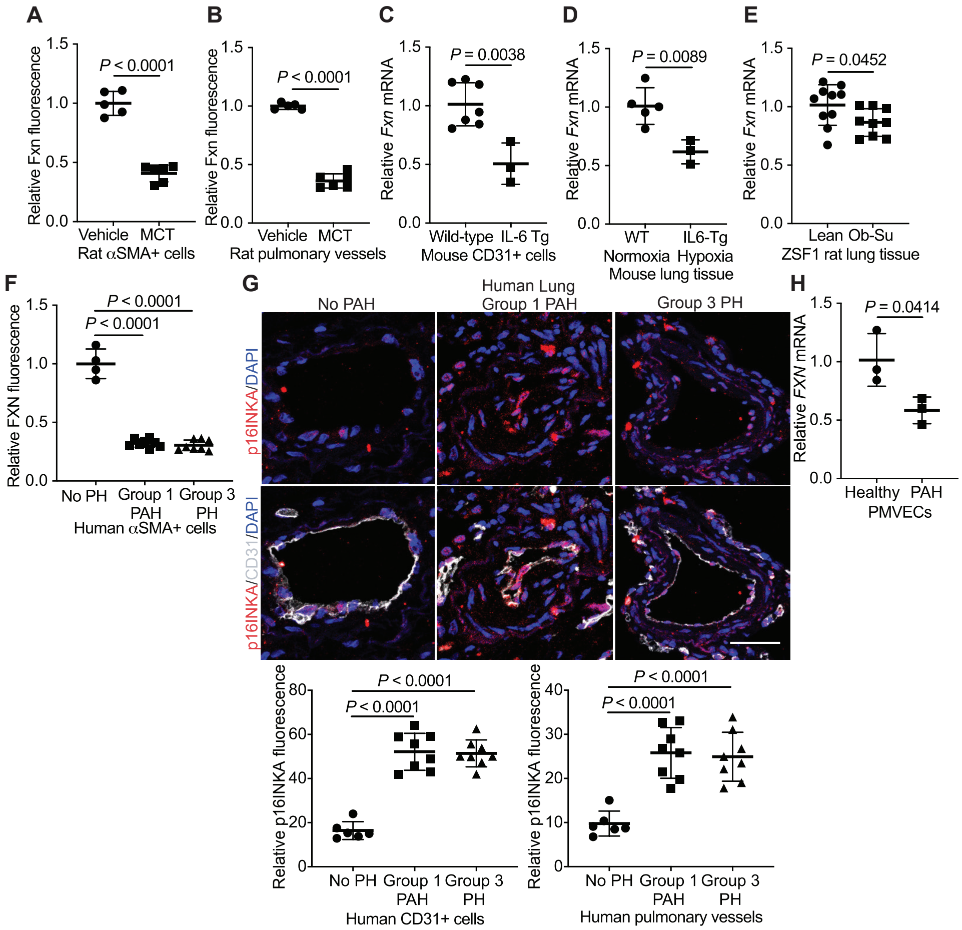

Supplemental Figure 1. FXN and p16^{INKA} expression in the pulmonary vasculature of Group 1, 2, and 3 PH models. (A and B) Fxn co-localized with pulmonary medial layer (α-SMA+) for Group 1 PAH monocrotaline-treated rats (n=6) versus vehicle control (n=5). (C and D) RT-qPCR of *Fxn* transcript expression in CD31+ lung cells from normoxic IL-6 Tg mice (n=3) or whole-lung tissue from hypoxic IL-6 Tg mice (n=3) versus normoxic wild type control (n=7 and n=5, respectively). (E) RT-qPCR of *Fxn* levels in whole-lung from Sugen (SU5416)-treated obese ZSF1 (n=9) versus lean rats (n=10). (F) FXN levels co-localized with α-SMA+ cells in Group 1 PAH (n=8) or Group 3 PH (n=8) lungs compared to control (No PH) (n=4). (G) Immunofluorescent staining of p16^{INK4} (red), CD31 (white), and DAPI (blue) and confocal microscopy of No PH (n=6), Group 1 PAH (n=8), or Group 3 PH patient lungs (n=8). Quantification of co-localized and whole-vessel senescence marker. Scale bar indicates 50μm. (H) *FXN* expression by RT-qPCR in pulmonary microvascular endothelial cells (PMVECs) from a patient with no PH compared to Group 1 PAH (n=3/group). Two-tailed Student's *t*-test (panels A-E, H) and one-way ANOVA and Tukey's post hoc analysis (panels F-G) with error bars that reflect mean +/- SD.

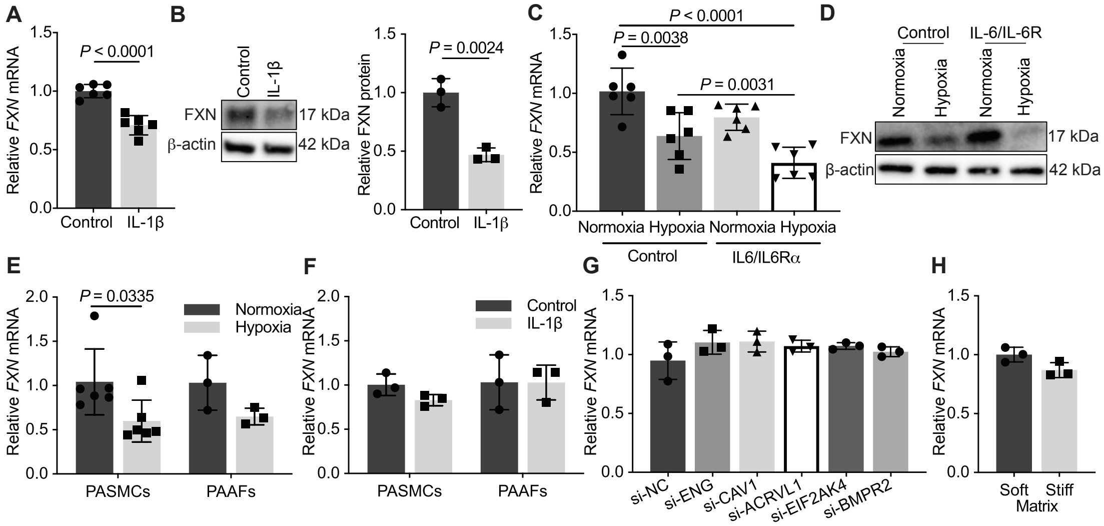

Supplemental Figure 2. FXN reduction in cultured pulmonary vascular cells. (A and B) RT-qPCR (n=6/group) and immunoblot (n=3/group) following IL-1β treatment (≥ 24 hours, 10 ng/ml) in pulmonary artery endothelial cells (PAECs). (C and D) FXN transcript and protein levels in PAECs exposed to normoxic or hypoxic conditions with or without IL-6/IL-6 receptor treatment (n=3/group). (E and F) RT-qPCR of *FXN* expression in cultured pulmonary artery smooth muscle cells (PASMCs, n=6) and adventitial fibroblasts (PAAFs, n=3) exposed to chronic hypoxia (≥ 24 hours, <1% O_2) or IL-1β (≥ 24 hours, 10ng/ml). (G) Pulmonary artery endothelial cell (PAEC) FXN mRNA levels following siRNA transfection of targets associated with mutations in PH (ENG, CAV1, ACRVL1, EIF2AK4, BMPR2) compared to negative control (NC) (n=3/group). (H) RT-qPCR of FXN transcript in PAECs seeded in soft (0.5 kPa) versus stiff matrix (50 kPa) for 48 hours (n=3/group). Two-tailed Student's *t*-test (panels A-B, E-F, H) and one-way ANOVA and Tukey's post hoc analysis (panels C and G) with error bars that reflect mean +/- SD.

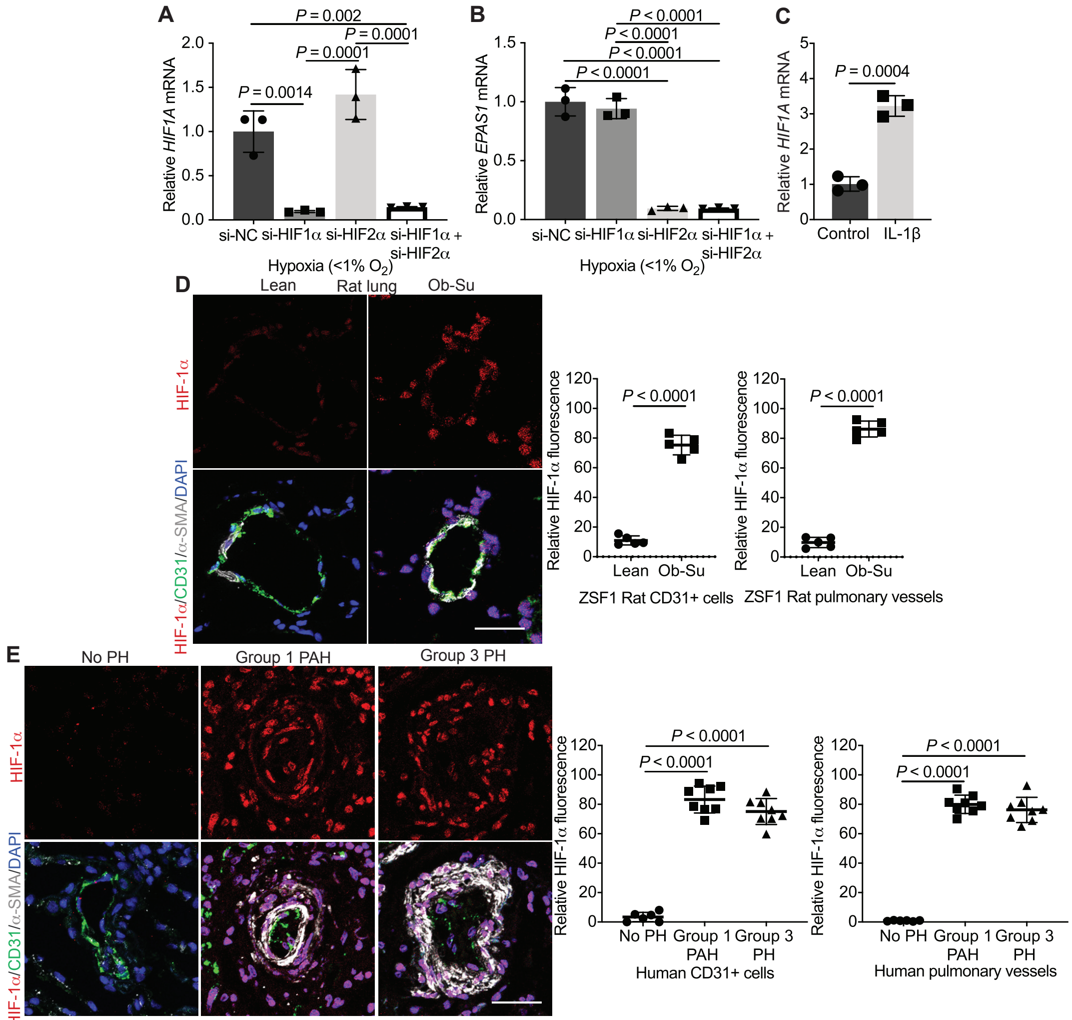

Supplemental Figure 3. HIF-α controls FXN across PH groups. (A and B) RT-qPCR of relative *HIF1A* and *EPAS1* levels for PAEC transfection control of HIF-1α, HIF-2α, or combined isoform-specific siRNA in hypoxic PAECs (n=3/group). (C) *HIF1A* transcript levels in IL-1β-treated PAECs compared to controls (n=3/group). (D and E) Immunofluorescent staining of HIF-1α (red), CD31 (green), α-SMA (gray), and counterstaining nuclei with DAPI (blue) followed by confocal microscopy. Scale bars denote 50μm. Quantification of HIF-1α levels colocalized in CD31+ cells and in the pulmonary vessels of (D) obese ZSF1 rats treated with Sugen (Ob-Su) compared to lean controls (n=5/group) and of (E) patients with Group 1 PAH (n=8), Group 3 PH (n=8) or no PH (n=6), respectively. Two-tailed Student's *t*-test (panels A-D) and one-way ANOVA and Tukey's post hoc analysis (panel E) with error bars that reflect mean +/- SD.

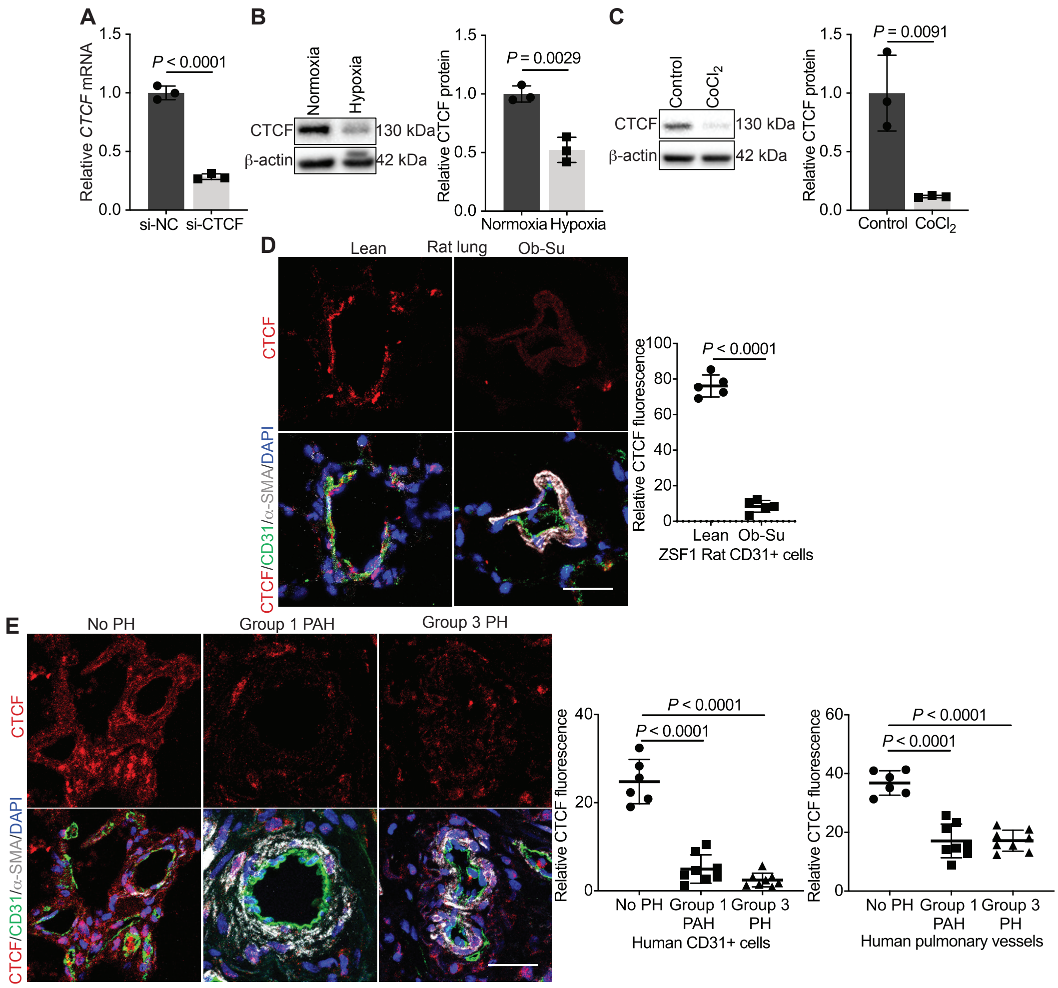

Supplemental Figure 4. Reduced CTCF in models of Group 1, 2, and 3 PH. (A) RT-qPCR of *CTCF* transcript for PAEC transfection control of CTCF siRNA. (B) Immunoblot of CTCF protein in hypoxic PAECs (≥ 24 hours, <1% O_2). (C) Immunoblot of CTCF protein in PAECs treated with $CoCl_2$ (≥ 24 hours, 750μM). (D and E) Immunofluorescent staining and confocal imaging of CTCF (red), α-SMA (gray), CD31 (green), and counterstaining with DAPI followed by confocal microscopy. Scale bars indicated 50μm. (D) Representative imaging and quantification of CTCF co-localized with the CD31 endothelium in obese, Sugen-treated (Ob-Su) versus lean rats (n=5/group). (E) CTCF levels in CD31+ cells and pulmonary vessels of lungs from patients with Group 1 PAH (n=8) or Group 3 PH (n=8) compared to no PH controls (n=6). Two-tailed Student's *t*-test (panels A-D) and one-way ANOVA and Tukey's post hoc analysis (panel E) with error bars that reflect mean +/- SD.

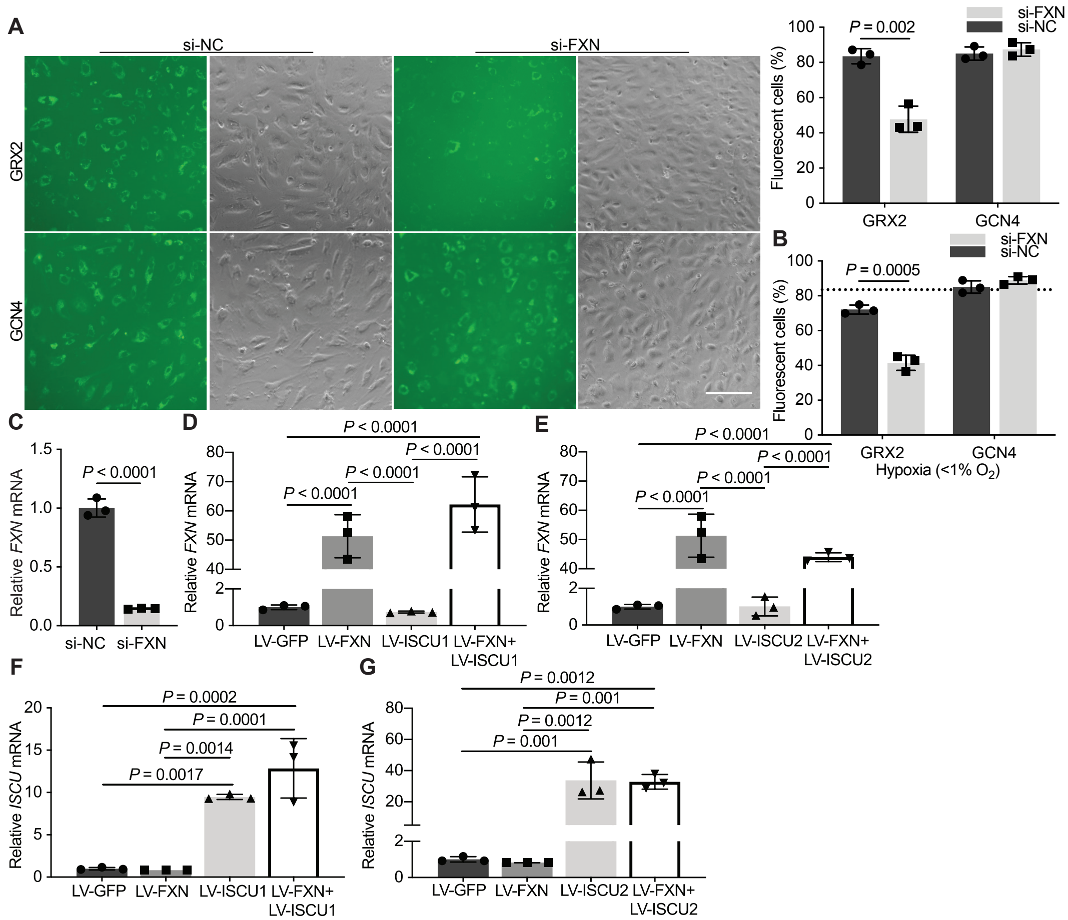

Supplemental Figure 5. Acute FXN knockdown in cultured pulmonary artery endothelial cells. (A) Representative images (scale bar indicates 400μm) and quantification of Fe-S cluster formation by fluorescent cell percentage in pulmonary artery endothelial cells (PAECs) transduced with glutaredoxin (GRX2) or GCN4 control constructs and transfected with FXN siRNA or negative control. (B) Fe-S-dependent fluorescence in hypoxic PAECs with and without FXN knockdown. Dotted line represents GRX2 mean fluorescence in normoxic control PAECs. (C) 48-hour transfection control for *FXN* transcript expression by RT-qPCR following siRNA knockdown in PAECs. (D-G) Efficiency of forced overexpression of *FXN* and *ISCU* transcripts with FXN, ISCU1, ISCU2, and combined lentiviruses compared to GFP control. Two-tailed Student's *t*-test (panels A-C) and one-way ANOVA and Tukey's post hoc analysis (panels D-G) with error bars that reflect mean +/- SD.

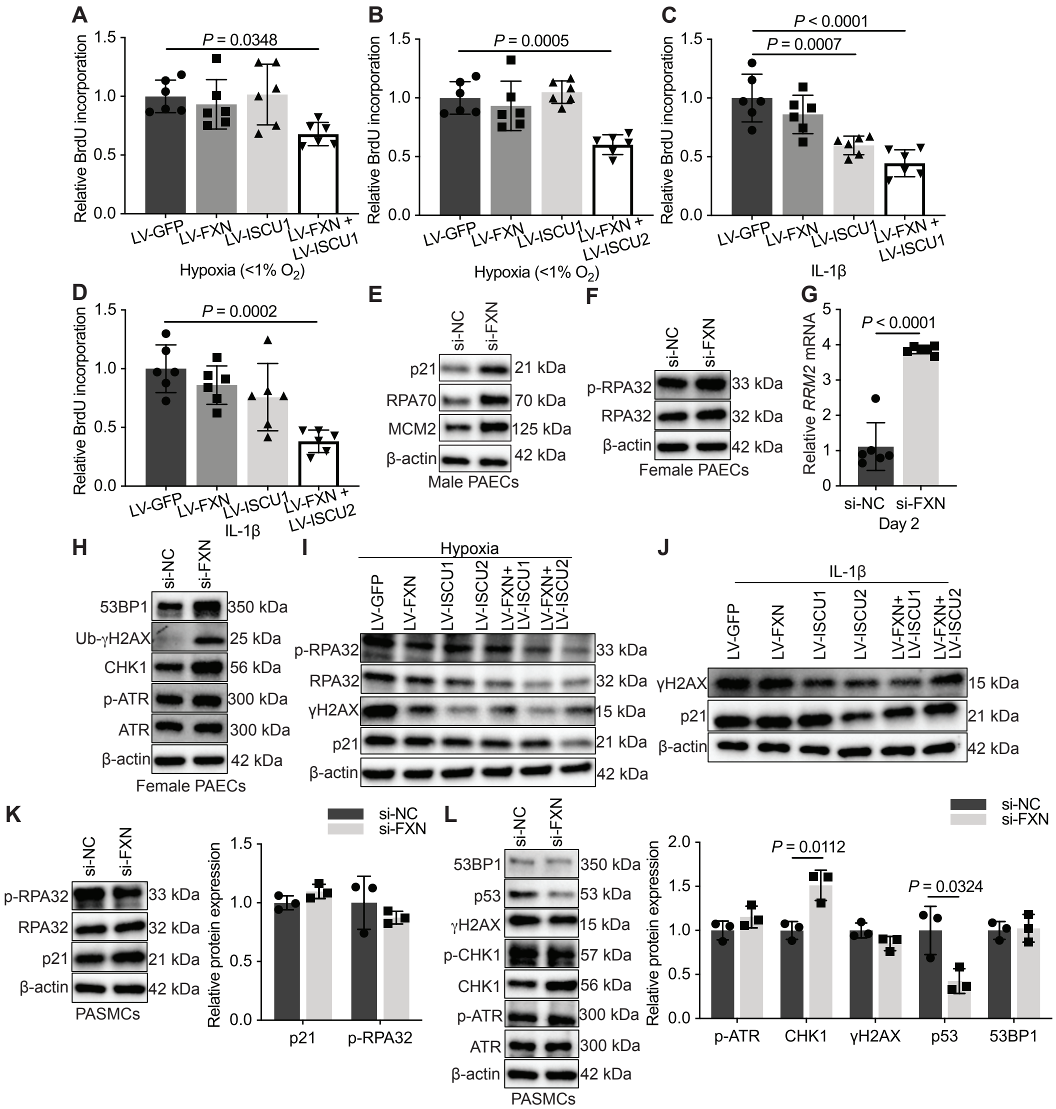

Supplemental Figure 6. FXN-dependent genotoxic stress in endothelial cells but not smooth muscle cells. (A-D) Colorimetric BrdU incorporation in (A and B) hypoxic and (C and D) IL-1β-treated PAECs after lentiviral transduction of FXN and/or ISCU1 and 2 (n=6/group). (E) Immunoblot of replication fork (MCM2, RPA70) and cell cycle (p21^{Cip1}) markers measured in PAECs 2 days after transfection with FXN siRNA or negative control. (F) Representative immunoblot of p-RPA32 protein levels in PAECs from a separate female donor. (G) *RRM2* transcript levels in PAECs 2 days after transfection with FXN siRNA or negative control (NC) (n=6/group). (H) Representative immunoblot of DNA damage response markers in FXN-deficient female PAECs. (I and J) Representative immunoblot of cell cycle (p21^{Cip1}) and replication stress (p-RPA32, γH2AX) markers in hypoxic and IL-1β-exposed PAECs with forced expression of FXN in combination with ISCU1/2. (K and L) Immunoblot evaluation of cell cycle arrest, replication stress, DDR markers in FXN-deficient or control pulmonary artery smooth muscle cells (PASMCs) (n=3/group). The same β-actin blot was used as a control between panels F and H as well as K and L. Two-tailed Student's *t*-test (panels G, K-L) and one-way ANOVA with Tukey's post hoc analysis (panels A-D) with error bars that reflect mean +/- SD.

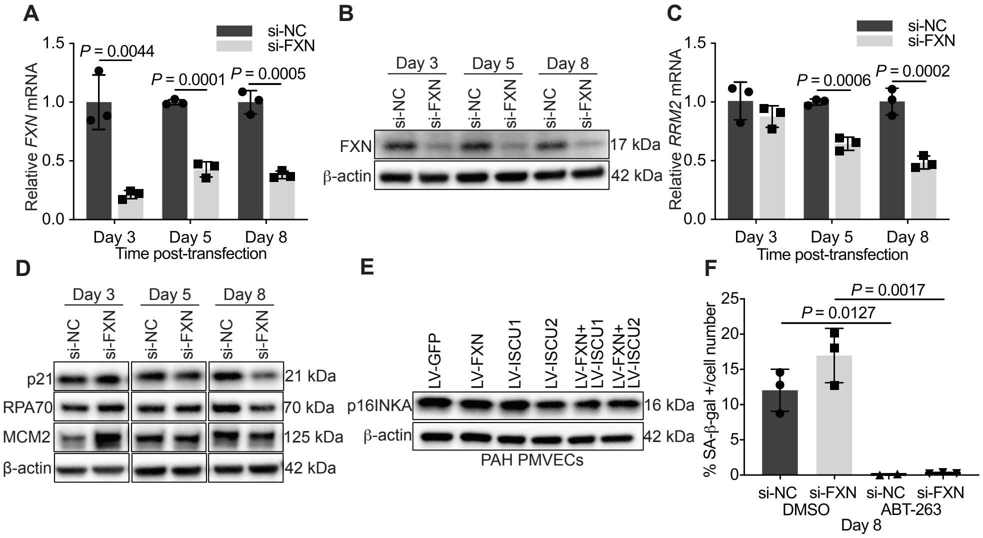

Supplemental Figure 7. FXN deficient-endothelial cells shift to DNA damage response-dependent senescence. (A and B) Transfection control RT-qPCR (n=3/group) and representative immunoblot in PAECs over a time course (day 3, 5, 8 post transfection). (C) *RRM2* mRNA expression day 3, day 5, and day 8 after transfection with FXN siRNA versus control (n=3/group). (D) Immunoblot of replication fork and cell cycle markers measured in transfected PAECs over a time course (day 3, 5, 8) (n=3/group). (E) p16^{INK4} protein levels following forced expression of FXN and ISCU1/2 in Group 1 PAH PMVECs. (F) Quantification of SA-β-gal staining in PAECs with FXN siRNA or negative control 8 days after transfection and treated with ABT-263 (24 hours, 0.25μM) or vehicle (n=3/group). Two-tailed Student's *t*-test (panels A, C) and two-way ANOVA and Tukey's post hoc analysis (panel F) with error bars that reflect mean +/- SD.

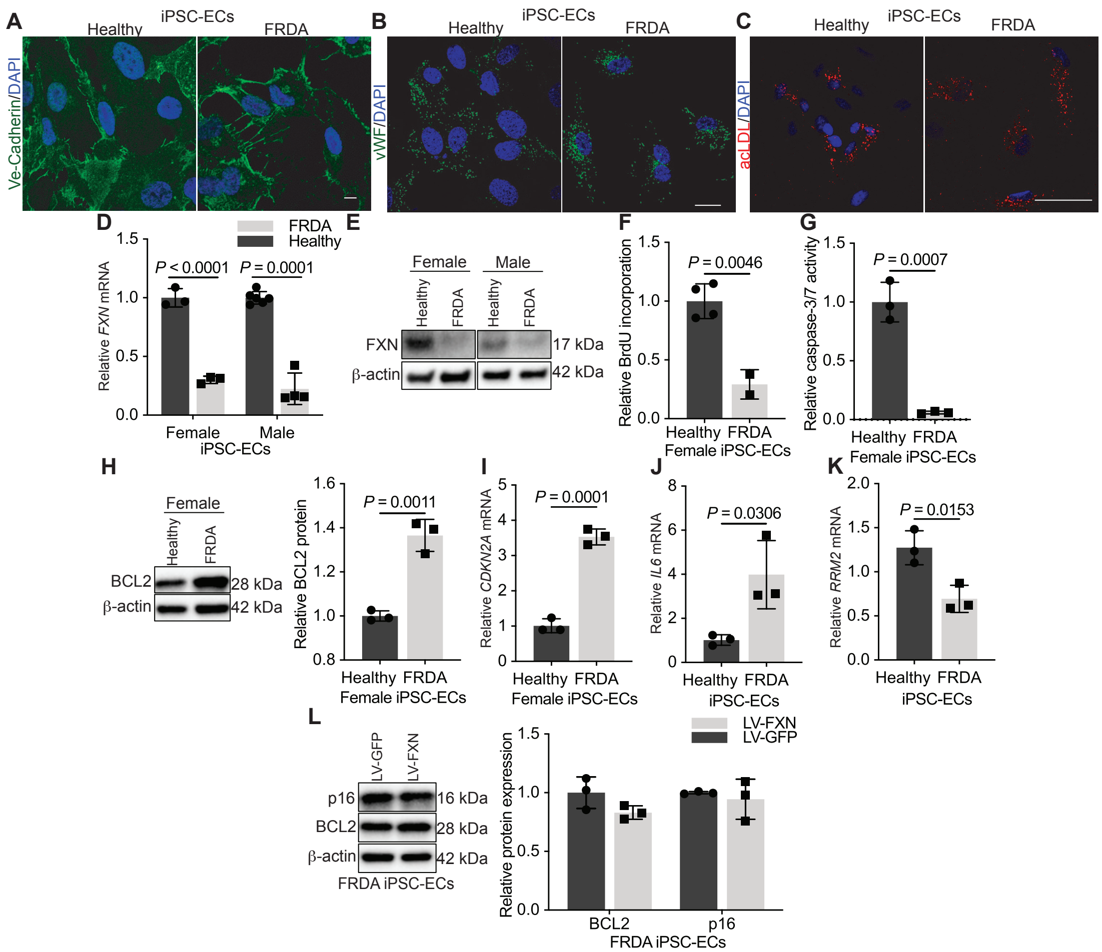

Supplemental Figure 8. Characterization of senescence in inducilbe pluripotent stem cell-derived endothelial cells from patients with Friedreich's ataxia. (A) Representative immunofluorescent staining and confocal imaging of Friedreich's ataxia (FRDA) and healthy inducible pluripotent stem cell-derived endothelial cells (iPSC-ECs) stained with endothelial marker VE-Cadherin (green) and counterstained with DAPI (blue). Scale bars indicate 10μm. (B) FRDA and healthy iPSC-ECs stained with vWF (green) and counterstained with DAPI (blue). Scale bars indicate 50μm. (C) Representative images of iPSC-EC uptake of fluorescent ac-LDL (red) and counterstained with DAPI (blue). Scale bars indicate 50μm. (D and E) RT-qPCR and immunoblot of FXN levels in age- and gender-matched FRDA iPSC-ECs compared to healthy controls. (F-I) Phenotypic experiments performed in female age-matched iPSC-ECs from healthy versus FRDA patients. (F) Replication measured by colorimetric BrdU incorporation assay (n=2-4). (G) Chemiluminescent caspase-3/7 activity. (H) BCL2 protein levels by immunoblot. (I) Relative *CDKN2A* mRNA expression. (J and K) *IL6* and *RRM2* transcript levels by RT-qPCR in male gender-matched iPSC-ECs. (L) Immunoblot of BCL2 and p16^{INKA} protein expression in male FRDA iPSC-ECs with forced overexpression via lentivirus of FXN (LV-FXN) compared to control (LV-GFP). Two-tailed Student's *t*-test unless otherwise specified with error bars that reflect mean +/- SD.

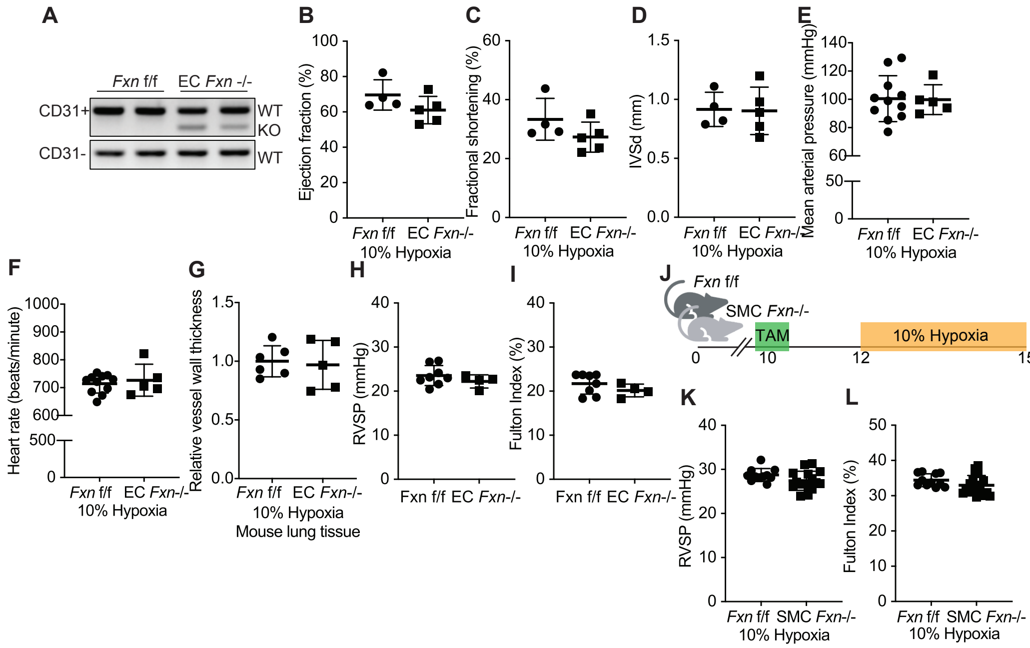

Supplemental Figure 9. Development of PH depends upon endothelial not smooth muscle FXN deficiency. (A-H) Experiments compare conditional EC *Fxn*-/- mice compared to *Fxn* f/f controls in normoxic or hypoxic conditions. (A) DNA gel of CD31+ and CD31- cells isolated from lungs of normoxic mice showing CD31-selective knockout of the floxed Fxn exon 4 (24), resulting in decreased Fxn expression. (B-D) Echocardiography of hypoxic mice measuring ejection fraction (%), fractional shortening (%), and interventricular septal end diastole (IVSd) width (mm) (n=4 versus n=5). (E) Tail cuff measurement of mean arterial pressure (mmHg) in hypoxic mice (n=11 versus n=5). (F) Heart rate (beats/minute) (n=11 versus n=5). (G) Quantification of relative vessel wall thickening measured by α-SMA in pulmonary arterioles of hypoxic EC *Fxn*-/- (n=5) mice compared to *Fxn* f/f controls (n=6). (H) Right ventricular systolic pressure (RVSP, mmHg) (n=8 versus n=4) in normoxic mice. (I) Fulton index (RV/LV+S, %) in normoxic mice (n=8 versus n=4). (J) Diagram of conditional smooth muscle cell (SMC) *Fxn*-/- (Myh11-ERT2+-Cre+) mice compared to *Fxn* f/f control exposed to chronic hypoxia (3 weeks, 10% hypoxia). (K) Right heart catheterization measuring RVSP (mmHg) in *Fxn* f/f (n=11) and SMC *Fxn*-/- (n=16) hypoxic mice. (L) Fulton index (%) (n=11 versus 16). Two-tailed Student's *t*-test was performed, with error bars that reflect mean +/- SD.

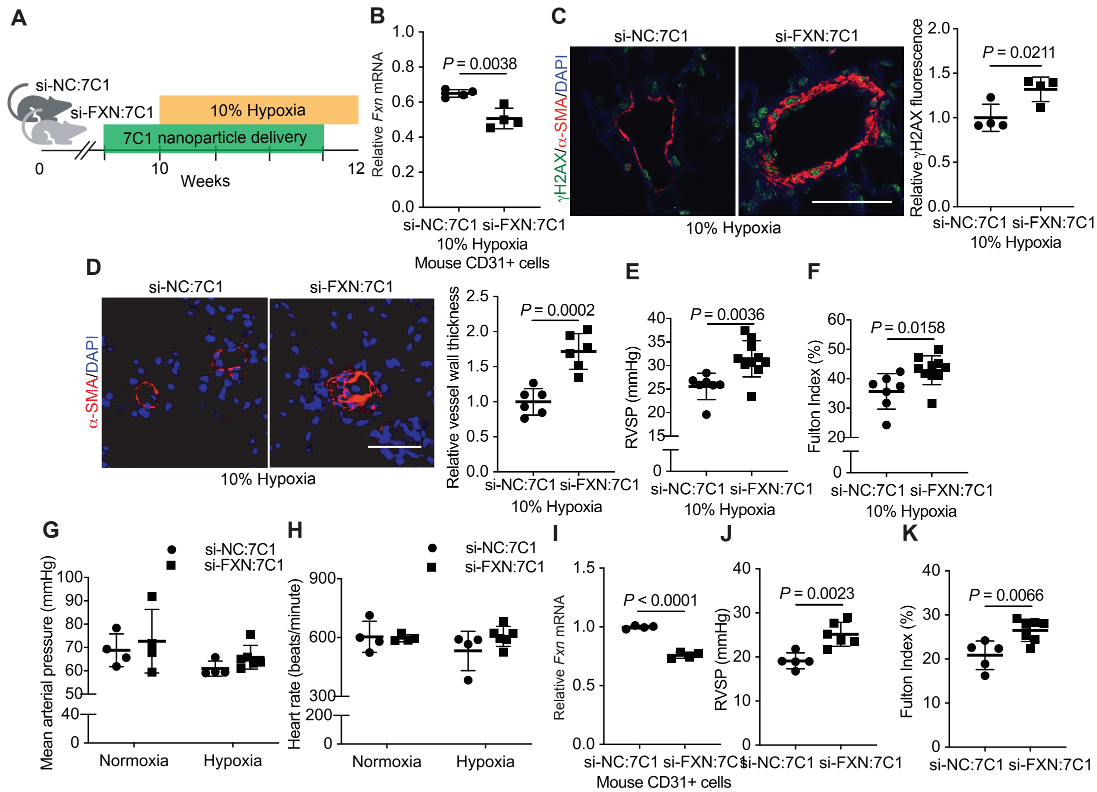

Supplemental Figure 10. Mice with pharmacologic FXN knockdown develop PH. (A) Experimental mouse model for pharmacologic Fxn knockdown. Endothelial delivery in male C57Bl6 using serial tail-vein injections of 7C1 nanoparticle containing Fxn (si-FXN:7C1) or negative control siRNA (si-NC:7C1) in hypoxic conditions (2 weeks, 10% O_2). (B) RT-qPCR of *Fxn* mRNA expression in CD31+ cells isolated from lungs (n=4/group). (C) Confocal microscopic imaging and quantification of pulmonary vascular γH2AX (green), α-SMA (red), and DAPI (blue) (n=4/group). Scale bars represent 50μm. (D) Relative medial thickening measured by immunofluorescent staining and confocal microscopic imaging of α-SMA (red) and DAPI (blue) in hypoxic mouse lungs (n=6/group). Scale bars represent 50μm. (E) Right heart catheterization measuring right ventricular systolic pressure (RVSP, mmHg) (n=7 versus n=10). (F) RV hypertrophy measured by Fulton index (RV/LV+S, %) (n=7 versus n= 10). (G) Tail cuff measuring mean arterial pressure in normoxic or hypoxic mice treated with negative control (n=4) or FXN siRNA (n=4-6). (H) Heart rate (beats/minute) (n=4-6/group). (I) In C57Bl6 mice treated with 7C1 nanoparticles containing Fxn (si-FXN:7C1) or negative control siRNA (si-NC:7C1) in normoxic conditions, RT-qPCR of Fxn mRNA expression in CD31+ cells isolated from lungs (n=4). (J) RVSP (mmHg) in normoxic mice (n=5 versus n=6). (K) Fulton index (%) in normoxic mice (n=5 versus n=7). Two-tailed Student's *t*-test (panels A-F, I-K) and two-way ANOVA and Tukey's post hoc analysis (panels G-H) with error bars that reflect mean +/- SD.

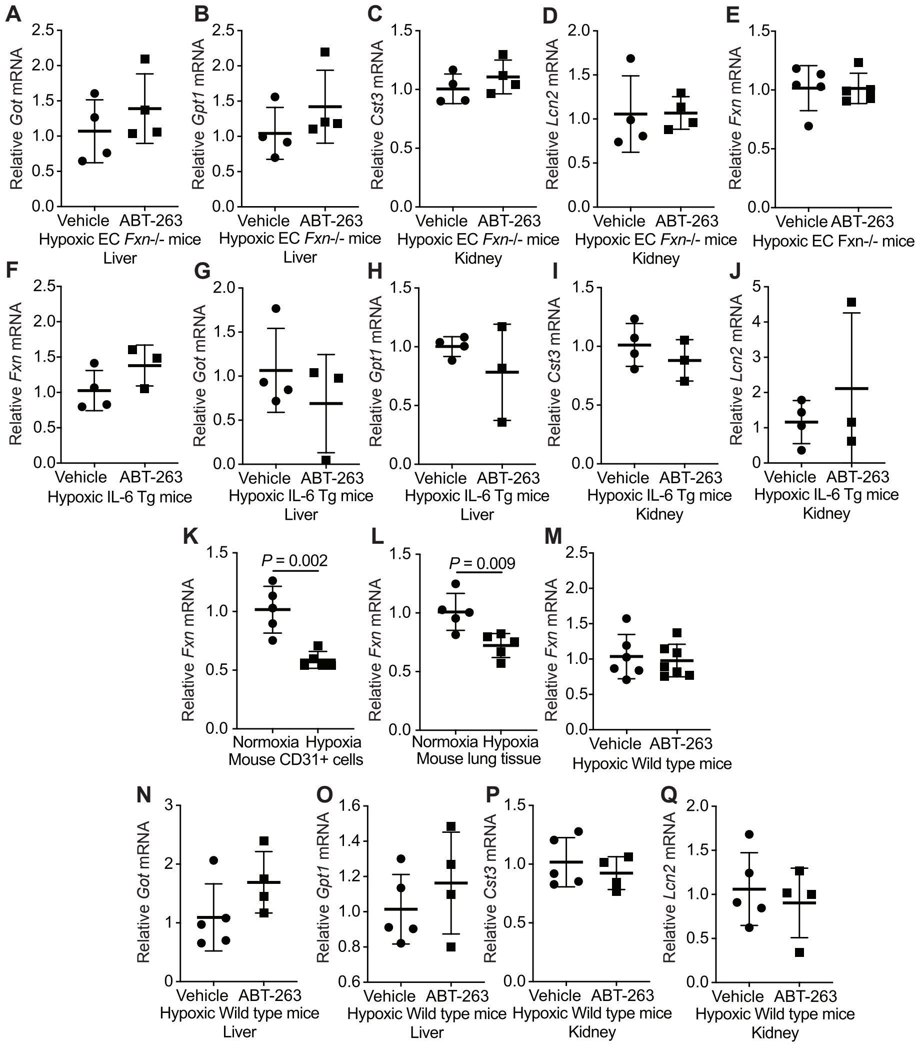

Supplemental Figure 11. Treatment of FXN-driven pulmonary vascular disease with the senolytic ABT-263. (A-E) Expression analysis via RT-qPCR in hypoxic (3 weeks, 10% O_2) endothelial-specific *Fxn*-/- mice treated with serial gavages of ABT-263 (25mg/kg/day) compared to vehicle control. (A and B) Transcript levels of mouse liver transaminases *Got* and *Gpt* to assess acute liver injury (n=4/group). (C and D) Transcript levels of acute kidney injury markers *Cst3* (34, 35) and *Lcn2* (36) (n=4/group). (E) Relative *Fxn* mRNA in mouse lung (n=5/group). (F-J) Transcript levels evaluated by RT-qPCR in male and female hypoxic (3 weeks, 10% O_2) IL-6 transgenic mice treated with a senolytic (n=3) or vehicle control (n=4). (F) *Fxn* mRNA in whole lung homogenates. (G and H) *Got* and *Gpt1* mRNA in liver homogenates. (I and J) *Cst3* and *Lcn2* mRNA in kidney homogenates. (K and L) *Fxn* levels in CD31+ cells or whole lung from C57BL/6 mice exposed to chronic hypoxia (10% O_2, 3 weeks) or normoxia (n=5/group). (M-Q) ABT-263 versus vehicle control treatment of wild type mice exposed to chronic hypoxia (3 weeks, 10% O_2). (M) RT-qPCR of *Fxn* levels in lung tissues (n=6 versus n=7). (N and O) Transcript expression of acute liver injury markers (n=5 versus n=4). (P and Q) Relative mRNA expression of acute kidney injury markers (n=5 versus n=4). Two-tailed Student's *t*-test with error bars that reflect mean +/- SD.

Supplemental References

1. Estephan LE, Genuardi MV, Kosanovich CM, Risbano MG, Zhang Y, Petro N, et al. Distinct plasma gradients of microRNA-204 in the pulmonary circulation of patients suffering from WHO Groups I and II pulmonary hypertension. *Pulm Circ.* 2019;9(2):2045894019840646.
2. Ku S, Soragni E, Campau E, Thomas EA, Altun G, Laurent LC, et al. Friedreich's ataxia induced pluripotent stem cells model intergenerational GAATTC triplet repeat instability. *Cell Stem Cell.* 2010;7(5):631-7.
3. Gu M, Shao NY, Sa S, Li D, Termglinchan V, Ameen M, et al. Patient-Specific iPSC-Derived Endothelial Cells Uncover Pathways that Protect against Pulmonary Hypertension in BMPR2 Mutation Carriers. *Cell Stem Cell.* 2017;20(4):490-504 e5.
4. Bertero T, Oldham WM, Cottrill KA, Pisano S, Vanderpool RR, Yu Q, et al. Vascular stiffness mechanoactivates YAP/TAZ-dependent glutaminolysis to drive pulmonary hypertension. *J Clin Invest.* 2016;126(9):3313-35.
5. Hoff KG, Culler SJ, Nguyen PQ, McGuire RM, Silberg JJ, and Smolke CD. In Vivo Fluorescent Detection of Fe-S Clusters Coordinated by Human GRX2. *Chemistry & Biology.* 2009;16(12):1299-308.
6. Yu Q, Tai YY, Tang Y, Zhao J, Negi V, Culley MK, et al. BOLA (BolA Family Member 3) Deficiency Controls Endothelial Metabolism and Glycine Homeostasis in Pulmonary Hypertension. *Circulation.* 2019;139(19):2238-55.
7. Saygin D, Tabib T, Bittar HET, Valenzi E, Sembrat J, Chan SY, et al. Transcriptional profiling of lung cell populations in idiopathic pulmonary arterial hypertension. *Pulm Circ.* 2020;10(1). Online ahead of print.
8. Zheng GX, Terry JM, Belgrader P, Ryvkin P, Bent ZW, Wilson R, et al. Massively parallel digital transcriptional profiling of single cells. *Nat Commun.* 2017;8:14049.
9. Butler A, Hoffman P, Smibert P, Papalexi E, and Satija R. Integrating single-cell transcriptomic data across different conditions, technologies, and species. *Nat Biotechnol.* 2018;36(5):411-20.
10. Hafemeister C, and Satija R. Normalization and variance stabilization of single-cell RNA-seq data using regularized negative binomial regression. *Genome Biol.* 2019;20(1):296.
11. Stuart T, Butler A, Hoffman P, Hafemeister C, Papalexi E, Mauck WM, 3rd, et al. Comprehensive Integration of Single-Cell Data. *Cell.* 2019;177(7):1888-902 e21.
12. Aran D, Looney AP, Liu L, Wu E, Fong V, Hsu A, et al. Reference-based analysis of lung single-cell sequencing reveals a transitional profibrotic macrophage. *Nat Immunol.* 2019;20(2):163-72.
13. Consortium EP. An integrated encyclopedia of DNA elements in the human genome. *Nature.* 2012;489(7414):57-74.
14. Martens JH, and Stunnenberg HG. BLUEPRINT: mapping human blood cell epigenomes. *Haematologica.* 2013;98(10):1487-9.
15. Patro R, Duggal G, Love MI, Irizarry RA, and Kingsford C. Salmon provides fast and bias-aware quantification of transcript expression. *Nat Methods.* 2017;14(4):417-9.
16. Anders S, and Huber W. Differential expression analysis for sequence count data. *Genome Biol.* 2010;11(10):R106.
17. Huang da W, Sherman BT, and Lempicki RA. Systematic and integrative analysis of large gene lists using DAVID bioinformatics resources. *Nat Protoc.* 2009;4(1):44-57.
18. Huang da W, Sherman BT, and Lempicki RA. Bioinformatics enrichment tools: paths toward the comprehensive functional analysis of large gene lists. *Nucleic Acids Res.* 2009;37(1):1-13.
19. The Gene Ontology C. Expansion of the Gene Ontology knowledgebase and resources. *Nucleic Acids Res.* 2017;45(D1):D331-D8.

20. Ashburner M, Ball CA, Blake JA, Botstein D, Butler H, Cherry JM, et al. Gene ontology: tool for the unification of biology. The Gene Ontology Consortium. *Nat Genet.* 2000;25(1):25-9.
21. Nieminuszczy J, Schwab RA, and Niedzwiedz W. The DNA fibre technique - tracking helicases at work. *Methods.* 2016;108:92-8.
22. Steiner MK, Syrkina OL, Kolliputi N, Mark EJ, Hales CA, and Waxman AB. Interleukin-6 overexpression induces pulmonary hypertension. *Circ Res.* 2009;104(2):236-44.
23. Lai YC, Tabima DM, Dube JJ, Hughan KS, Vanderpool RR, Goncharov DA, et al. SIRT3-AMP-Activated Protein Kinase Activation by Nitrite and Metformin Improves Hyperglycemia and Normalizes Pulmonary Hypertension Associated With Heart Failure With Preserved Ejection Fraction. *Circulation.* 2016;133(8):717-31.
24. Puccio H, Simon D, Cossee M, Criqui-Filipe P, Tiziano F, Melki J, et al. Mouse models for Friedreich ataxia exhibit cardiomyopathy, sensory nerve defect and Fe-S enzyme deficiency followed by intramitochondrial iron deposits. *Nat Genet.* 2001;27(2):181-6.
25. Wang Y, Nakayama M, Pitulescu ME, Schmidt TS, Bochenek ML, Sakakibara A, et al. Ephrin-B2 controls VEGF-induced angiogenesis and lymphangiogenesis. *Nature.* 2010;465(7297):483-6.
26. Wirth A, Benyo Z, Lukasova M, Leutgeb B, Wettschureck N, Gorbey S, et al. G12-G13-LARG-mediated signaling in vascular smooth muscle is required for salt-induced hypertension. *Nat Med.* 2008;14(1):64-8.
27. Chang J, Wang Y, Shao L, Laberge RM, Demaria M, Campisi J, et al. Clearance of senescent cells by ABT263 rejuvenates aged hematopoietic stem cells in mice. *Nat Med.* 2016;22(1):78-83.
28. Tse C, Shoemaker AR, Adickes J, Anderson MG, Chen J, Jin S, et al. ABT-263: A Potent and Orally Bioavailable Bcl-2 Family Inhibitor. *Cancer Res.* 2008;68(9):3421-8.
29. Dahlman JE, Barnes C, Khan OF, Thiriot A, Jhunjunwala S, Shaw TE, et al. In vivo endothelial siRNA delivery using polymeric nanoparticles with low molecular weight. *Nat Nano.* 2014;9(8):648-55.
30. White K, Lu Y, Annis S, Hale AE, Chau BN, Dahlman JE, et al. Genetic and hypoxic alterations of the microRNA-210-ISCU1/2 axis promote iron-sulfur deficiency and pulmonary hypertension. *EMBO Mol Med.* 2015;7(6):695-713.
31. Bertero T, Lu Y, Annis S, Hale A, Bhat B, Saggar R, et al. Systems-level regulation of microRNA networks by miR-130/301 promotes pulmonary hypertension. *J Clin Invest.* 2014;124(8):3514-28.
32. Bertero T, Cottrill KA, Lu Y, Haeger CM, Dieffenbach P, Annis S, et al. Matrix Remodeling Promotes Pulmonary Hypertension through Feedback Mechanoactivation of the YAP/TAZ-miR-130/301 Circuit. *Cell Rep.* 2015;13(5):1016-32.
33. Steiner MK, Syrkina OL, Kolliputi N, Mark EJ, Hales CA, and Waxman AB. Interleukin-6 overexpression induces pulmonary hypertension. *Circ Res.* 2009;104(2):236-44.
34. Song S, Meyer M, Türk TR, Wilde B, Feldkamp T, Assert R, et al. Serum cystatin C in mouse models: a reliable and precise marker for renal function and superior to serum creatinine. *Nephrol Dial Transplant.* 2009;24(4):1157-61.
35. Soto K, Coelho S, Rodrigues B, Martins H, Frade F, Lopes S, et al. Cystatin C as a marker of acute kidney injury in the emergency department. *Clin J Am Soc Nephrol.* 2010;5(10):1745-54.
36. Viau A, El Karoui K, Laouari D, Burtin M, Nguyen C, Mori K, et al. Lipocalin 2 is essential for chronic kidney disease progression in mice and humans. *J Clin Invest.* 2010;120(11):4065-76.

Full unedited gel for Figure 1E

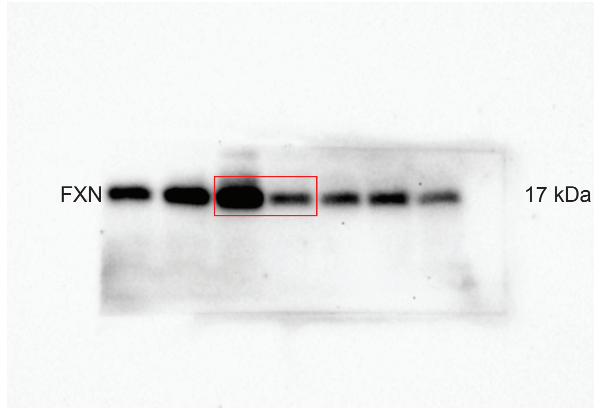

Full unedited gel for Figure 2A

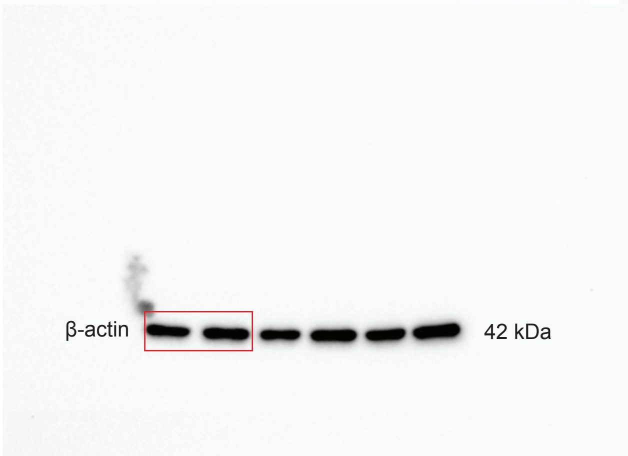

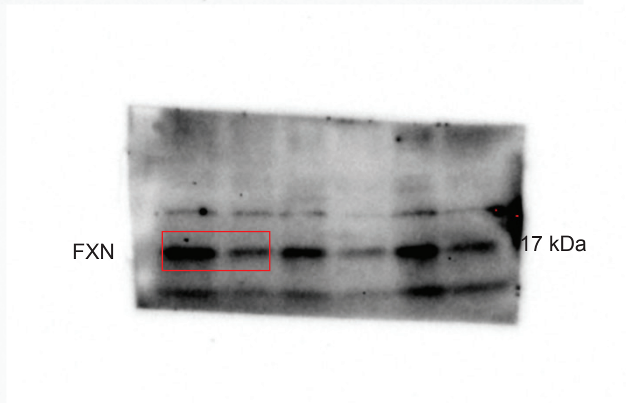

Full unedited gel for Figure 2B

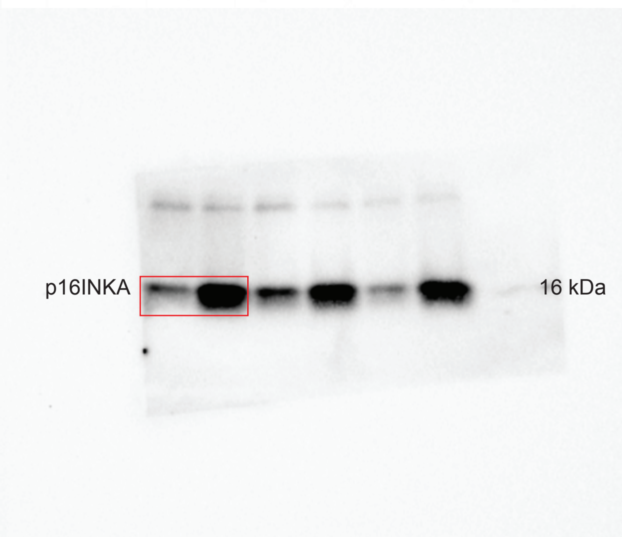

Full unedited gel for Figure 3B

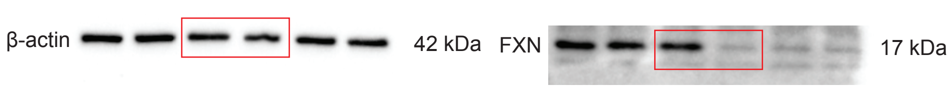

Full unedited gel for Figure 3D

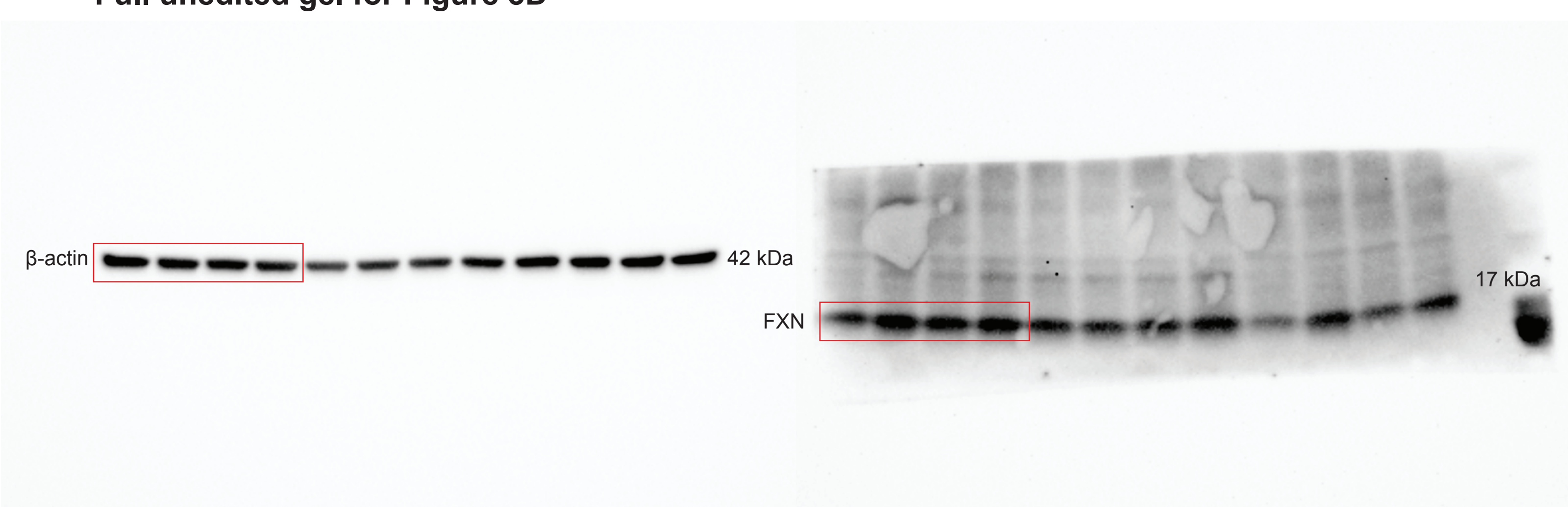

Full unedited gel for Figure 3F

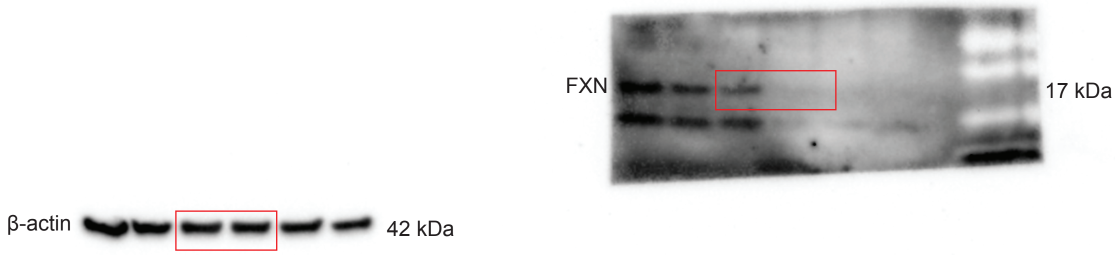

Full unedited gel for Figure 3G

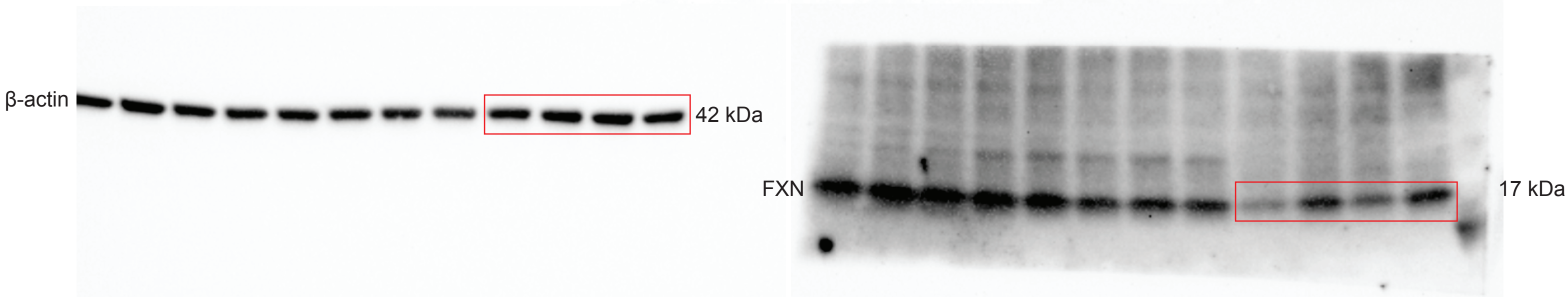

Full unedited gel for Figure 3I

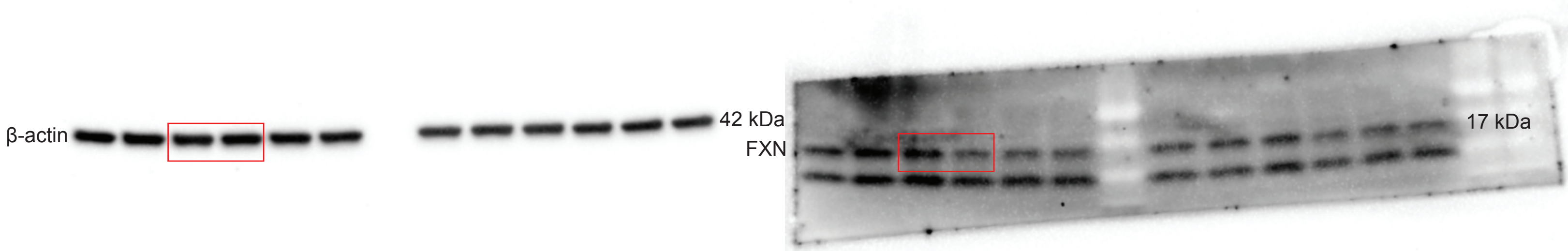

Full unedited gel for Figure 3J

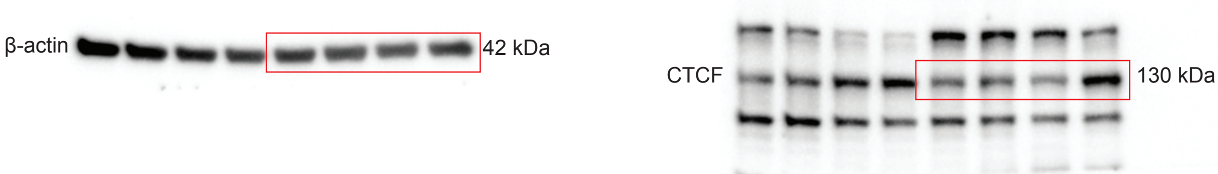

Full unedited gel for Figure 5D

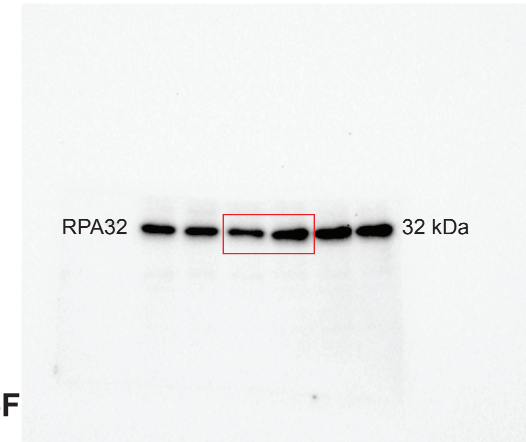

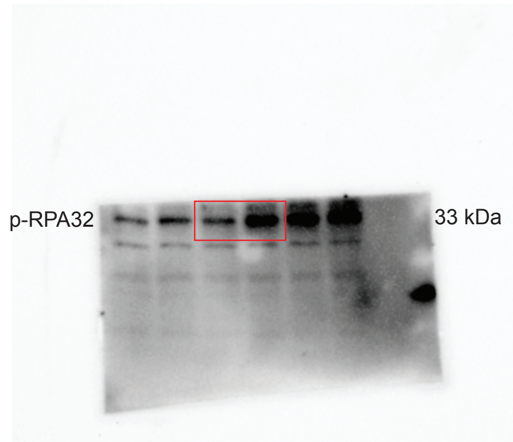

Full unedited gel for Figure 5F

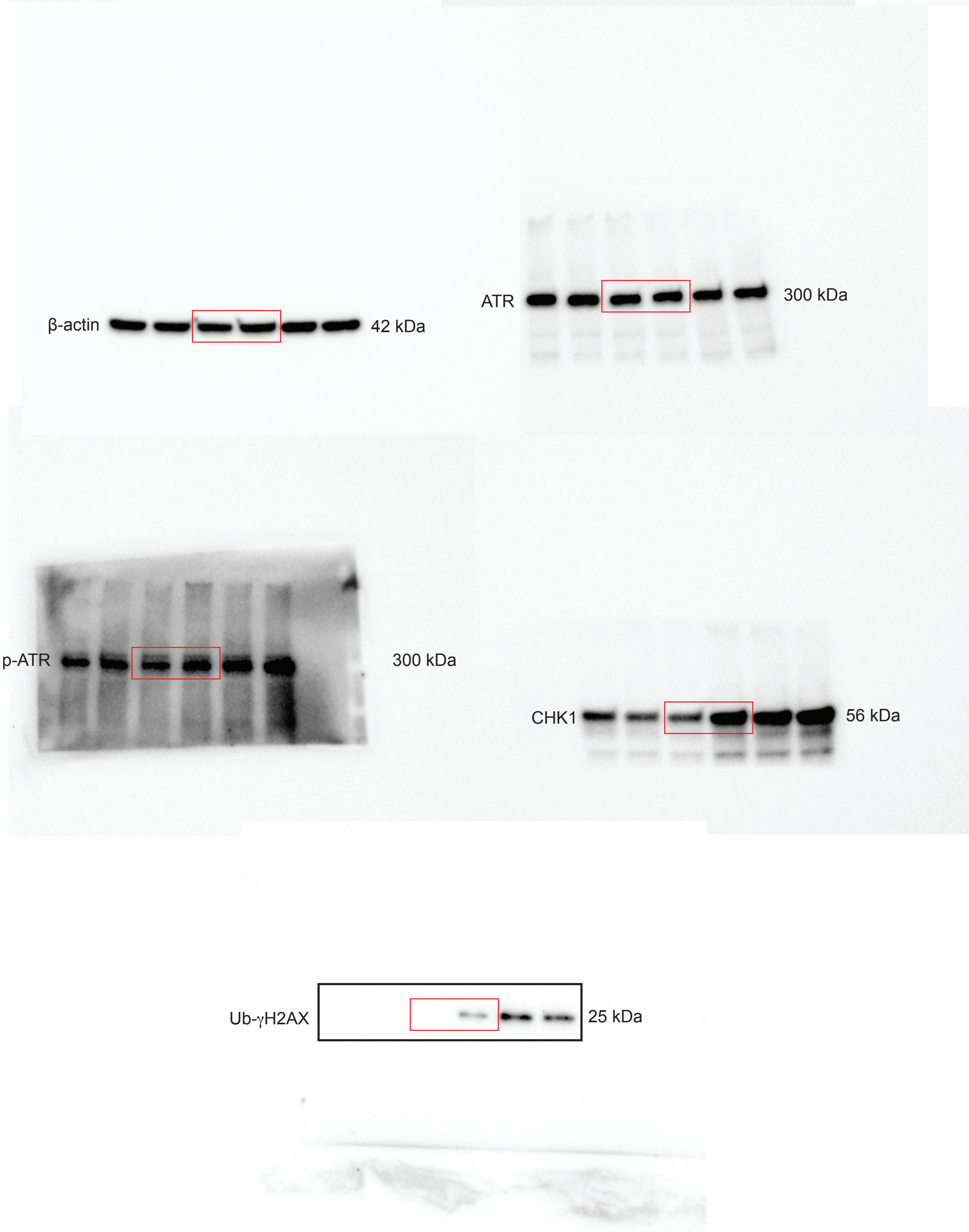

Full unedited gel for Figure 6C

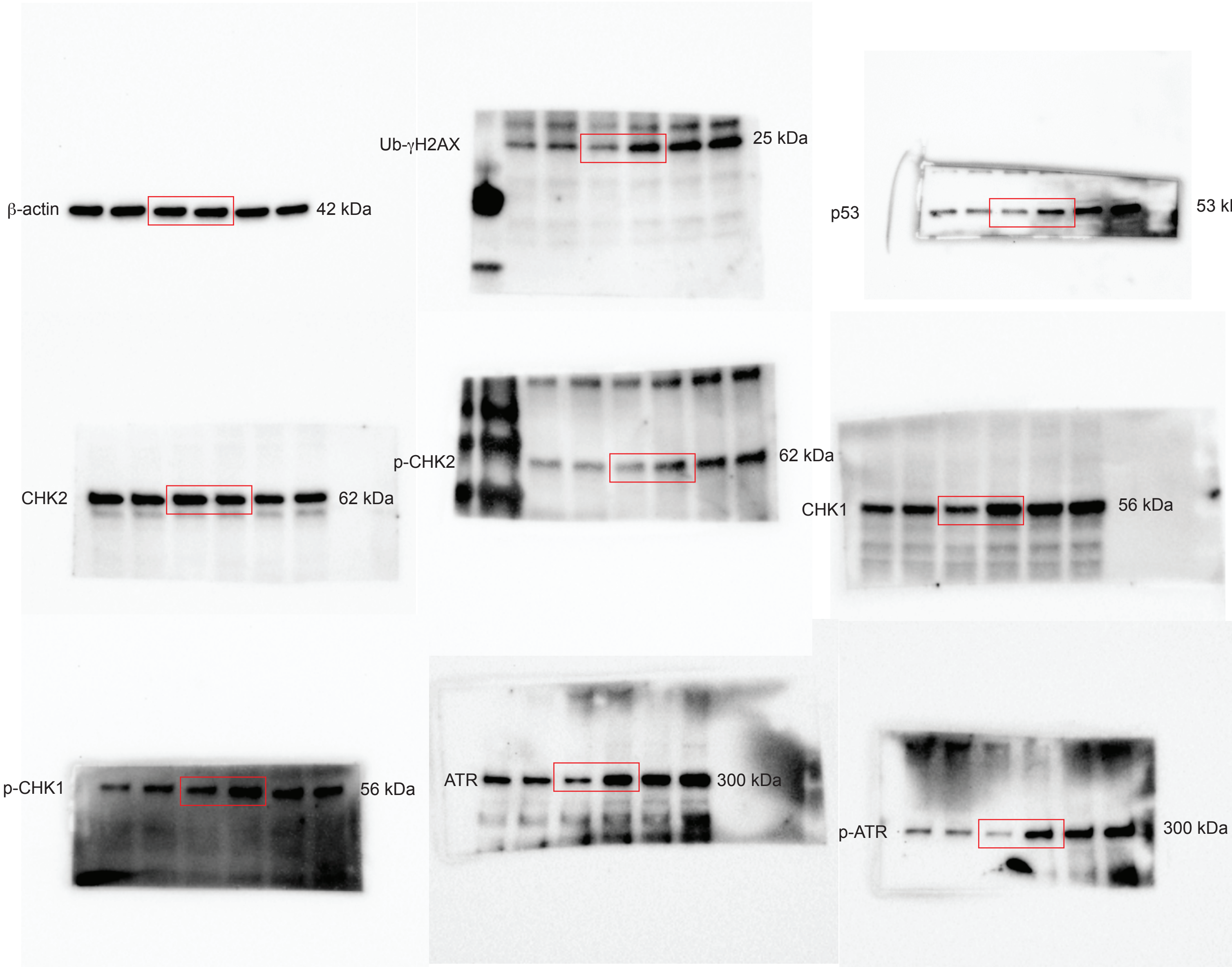

Full unedited gel for Figure 6D

Full unedited gel for Figure 7D and F

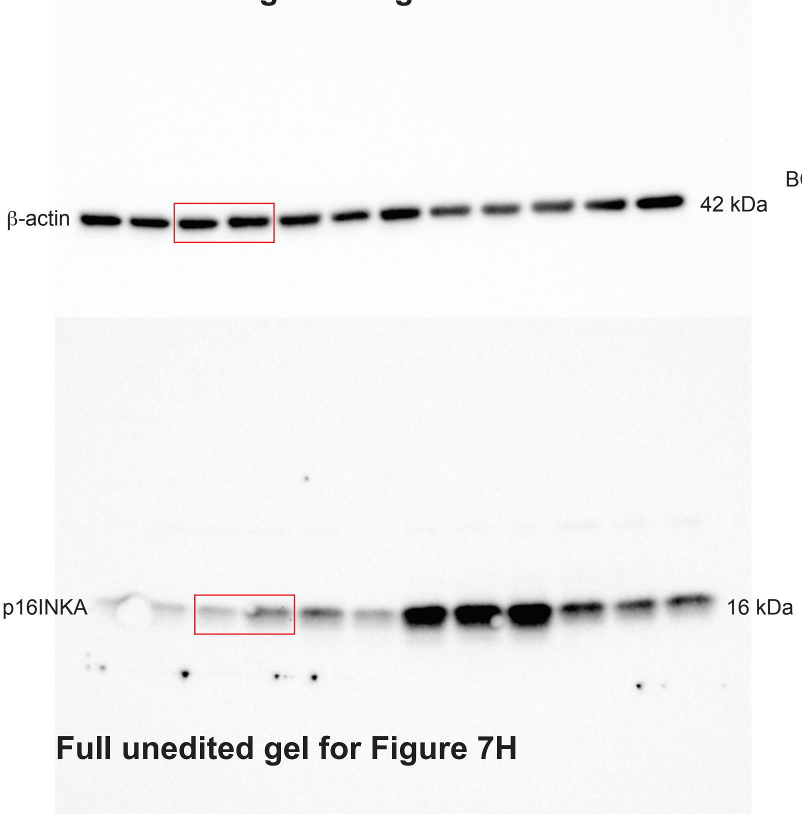

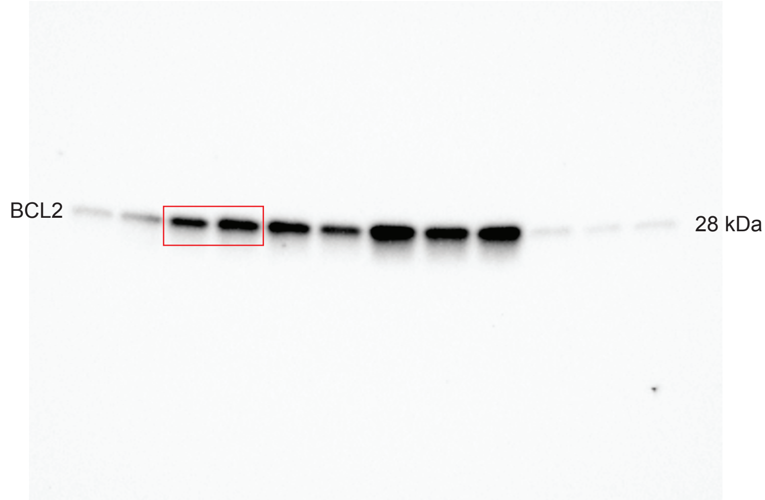

Full unedited gel for Figure 7H

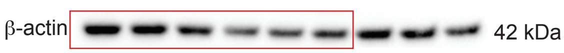

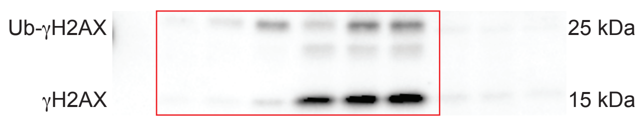

Full unedited gel for Supplemental Figure 2B

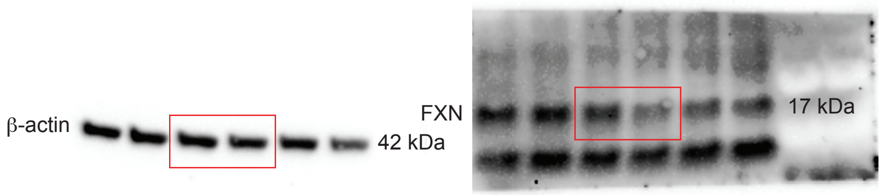

Full unedited gel for Supplemental Figure 2D

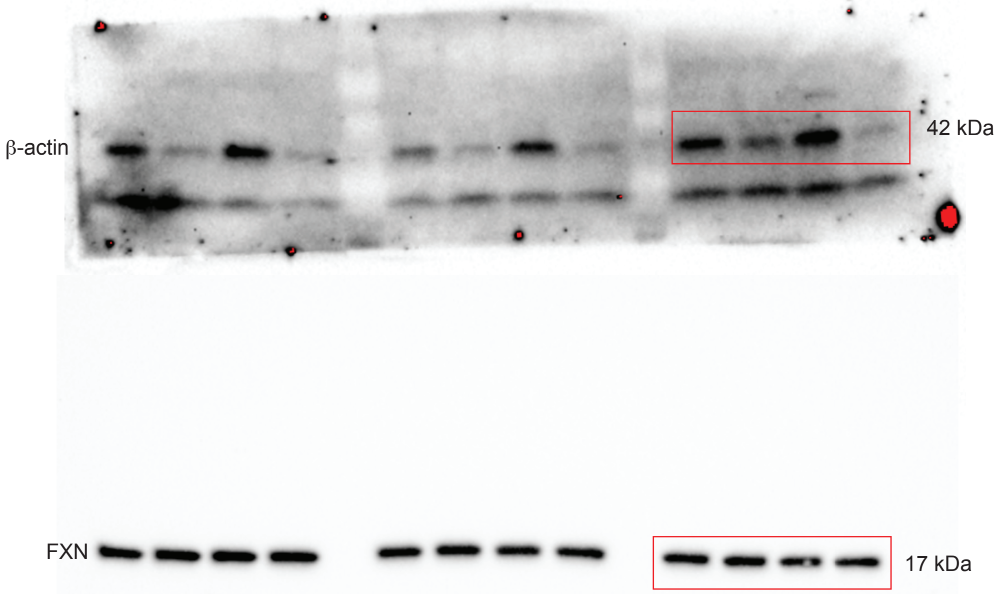

Full unedited gel for Supplemental Figure 4B

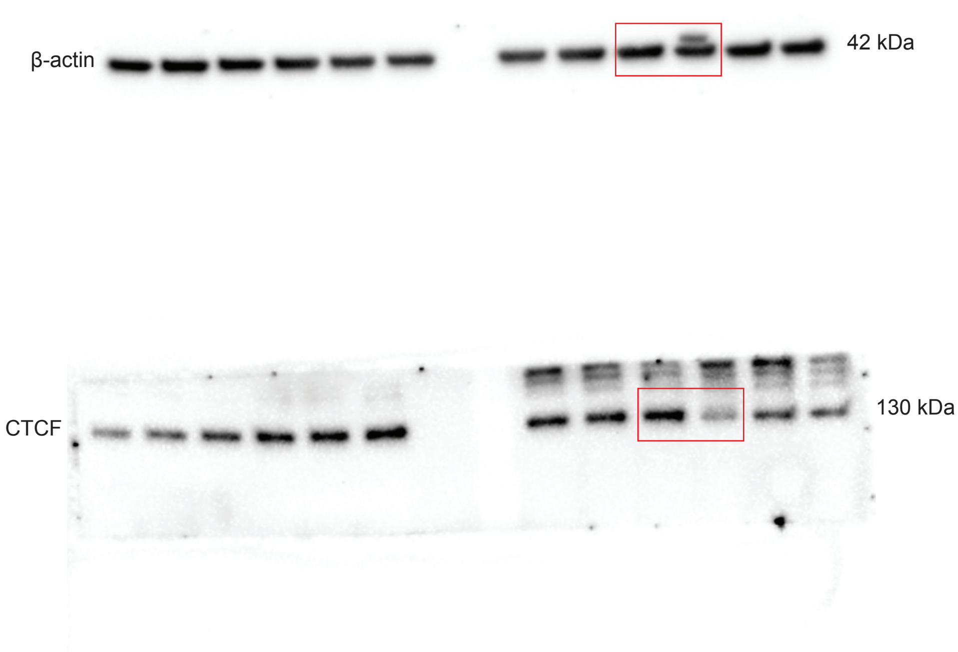

Full unedited gel for Supplemental Figure 4C

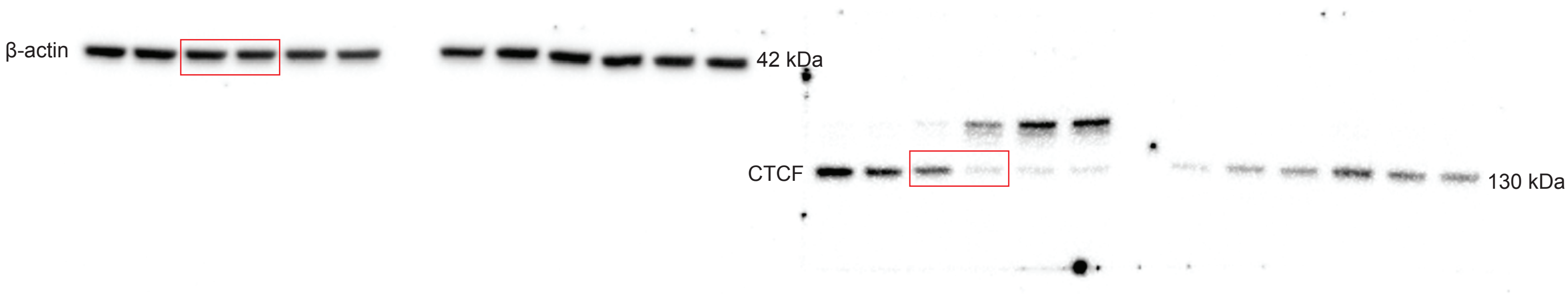

Full unedited gel for Supplemental Figure 6E

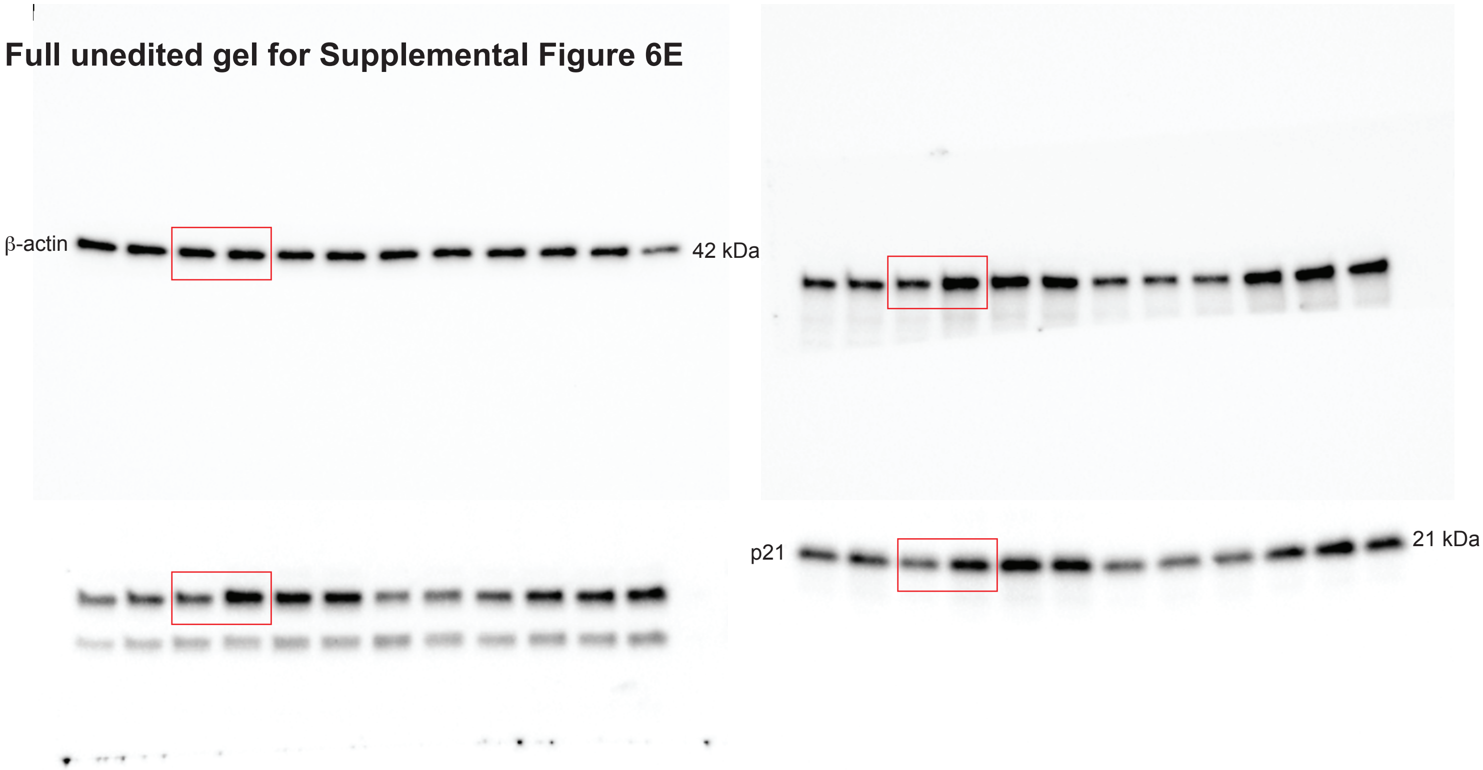

Full unedited gel for Supplemental Figure 6F and H

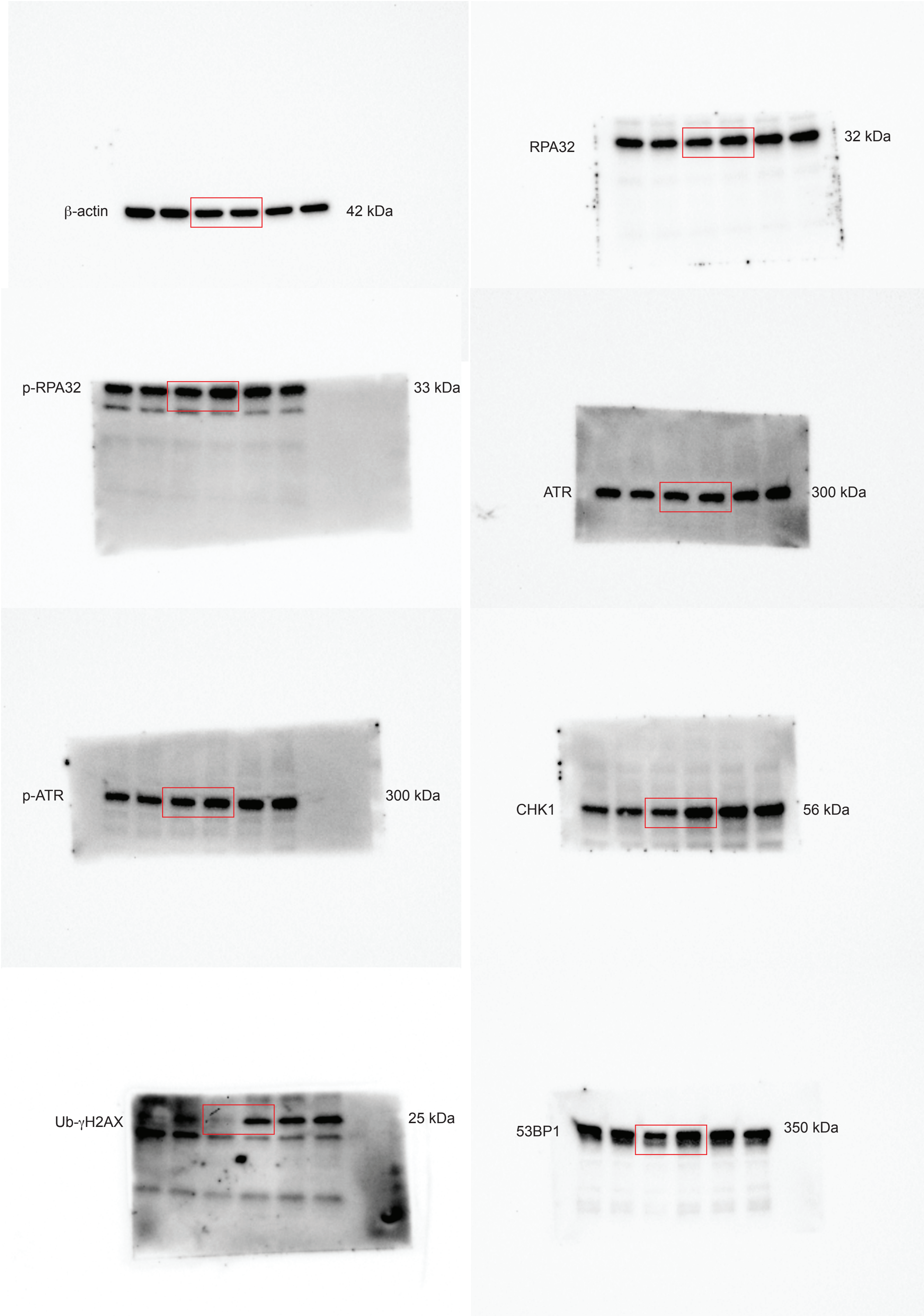

Full unedited gel for Supplemental Figure 6I

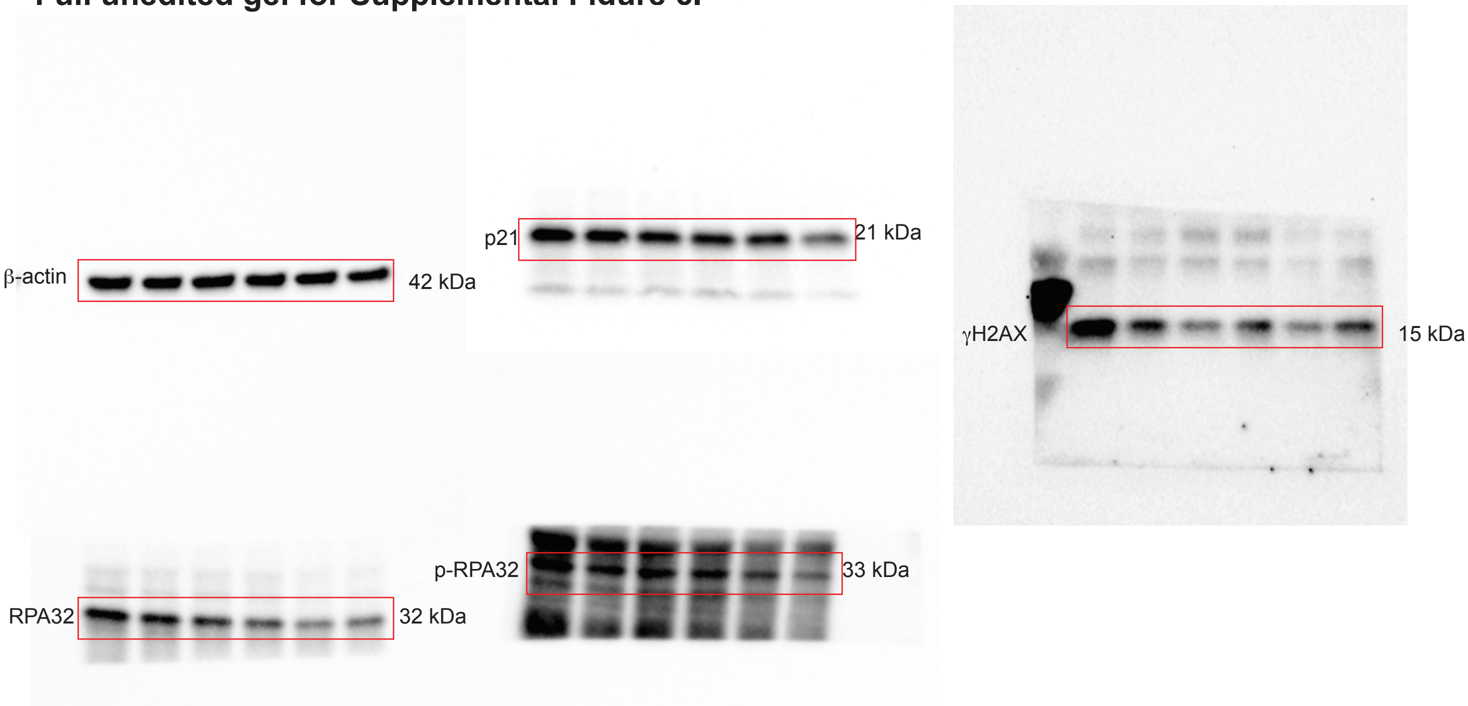

Full unedited gel for Supplemental Figure 6J

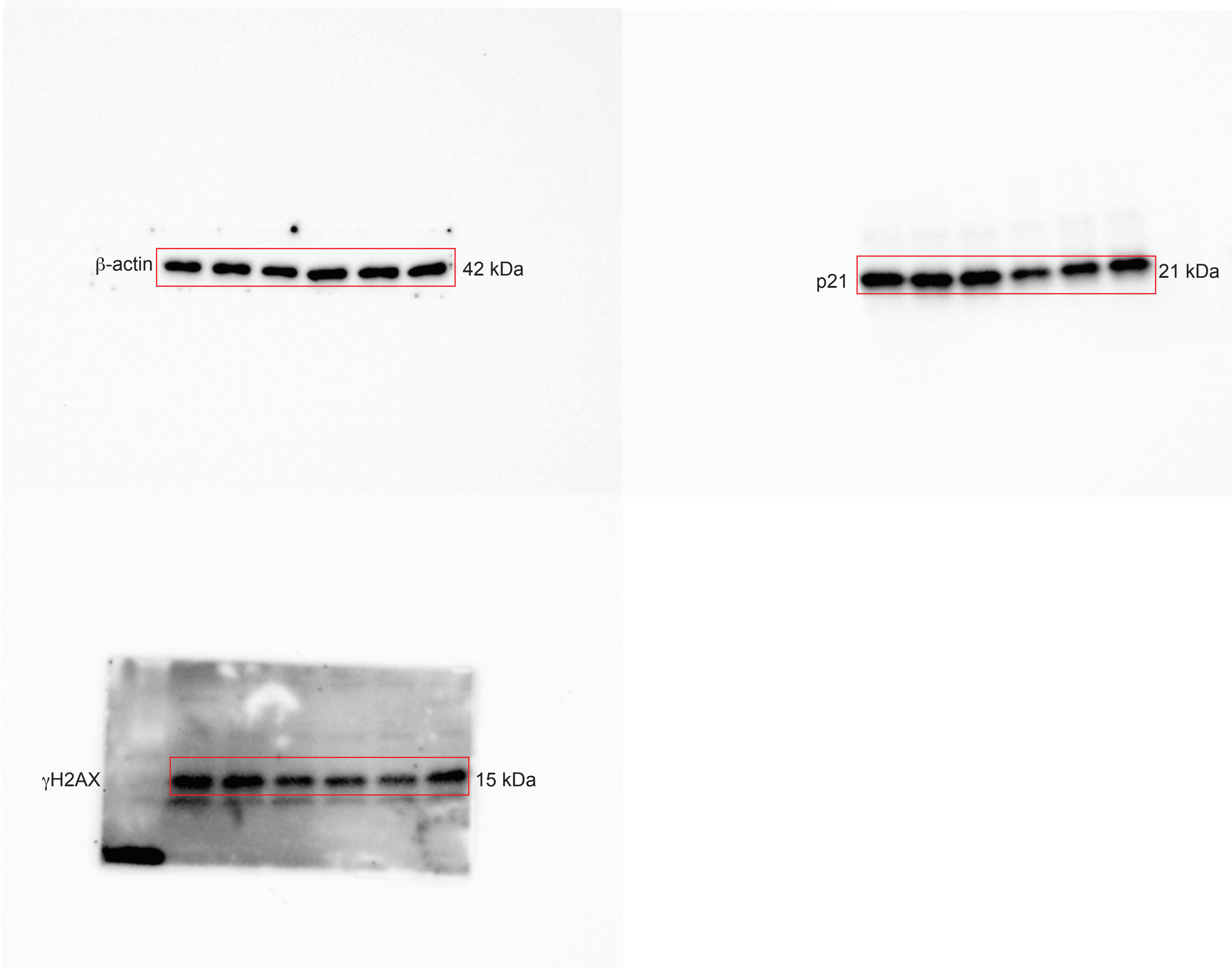

Full unedited gel for Supplemental Figure 6K and L

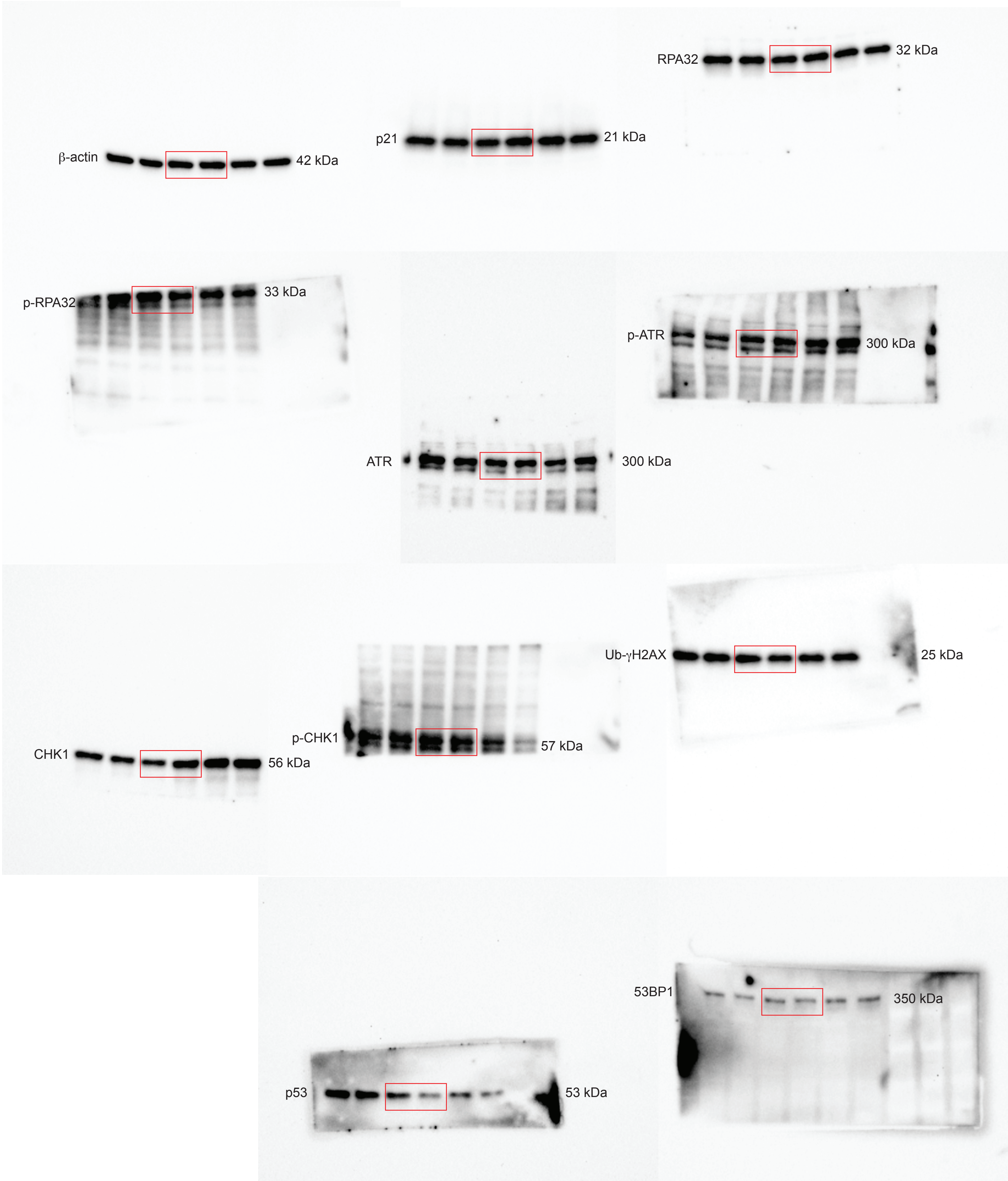

Full unedited gel for Supplemental Figure 7B

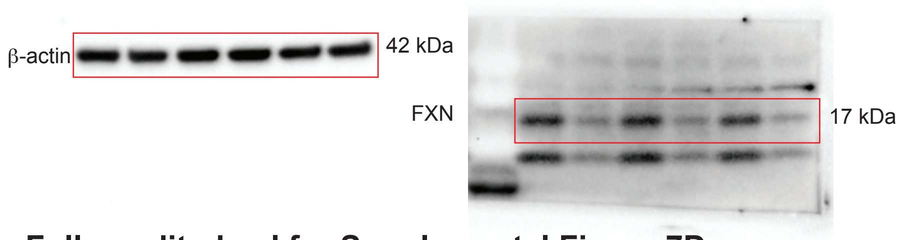

Full unedited gel for Supplemental Figure 7D

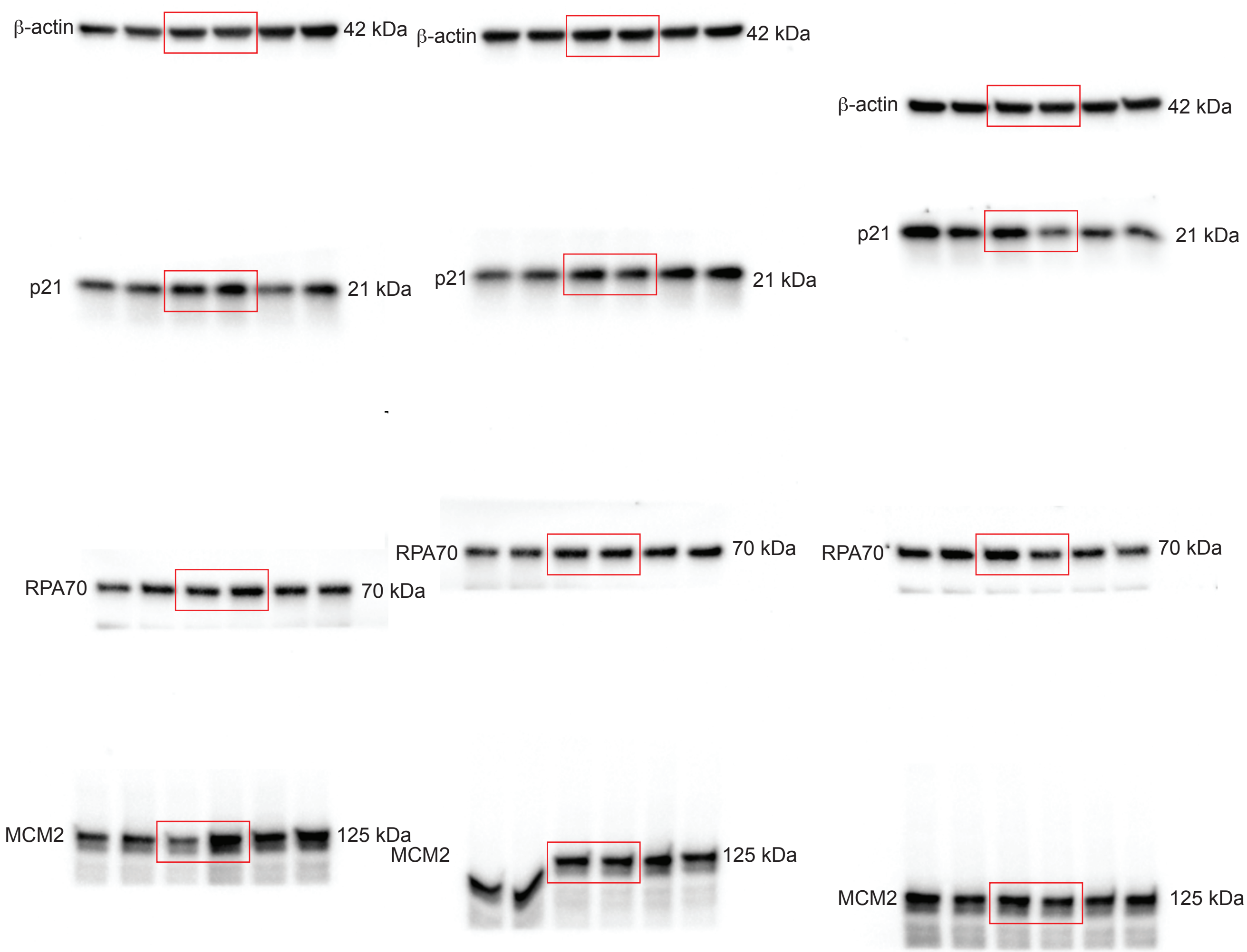

Full unedited gel for Supplemental Figure 7D

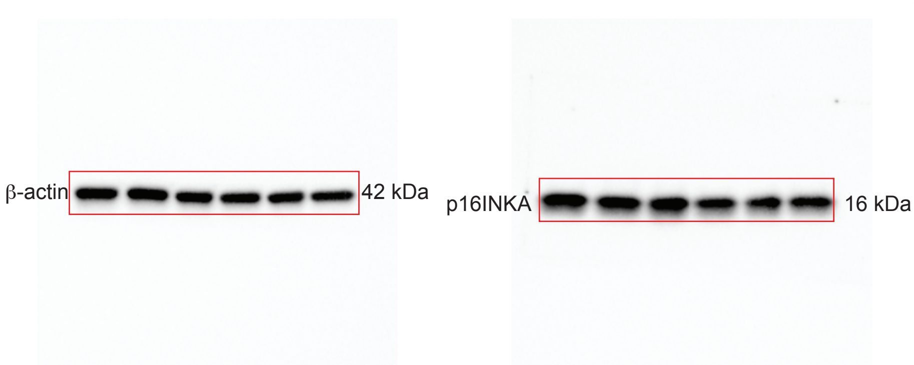

Full unedited gel for Supplemental Figure 8E

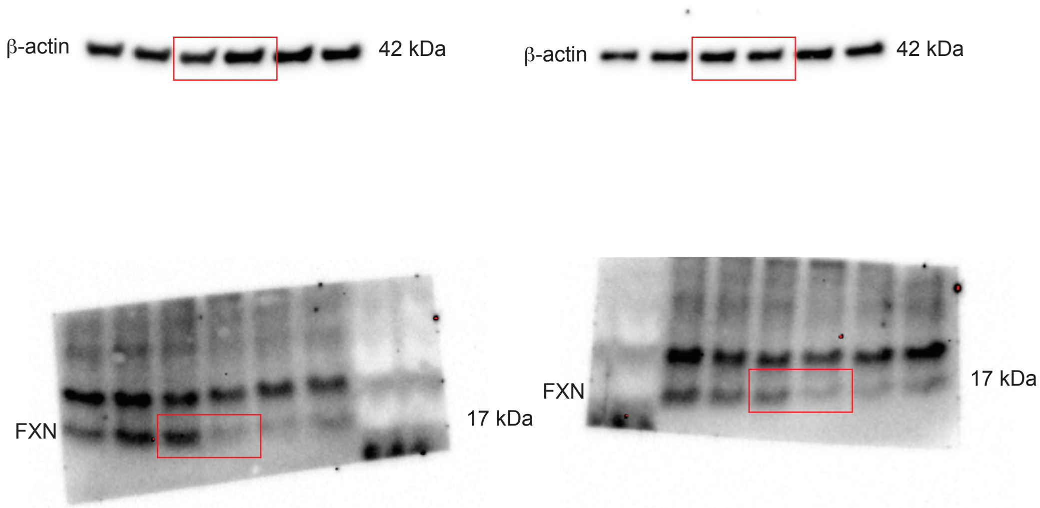

Full unedited gel for Supplemental Figure 8H

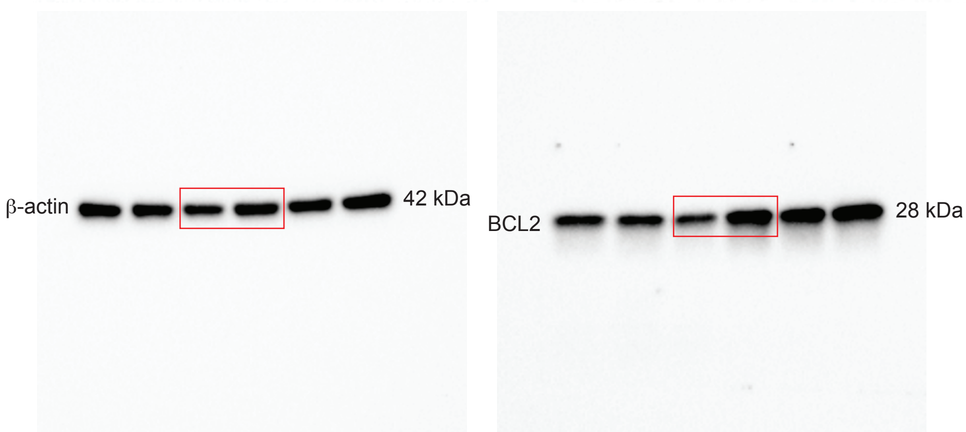

Full unedited gel for Supplemental Figure 8L

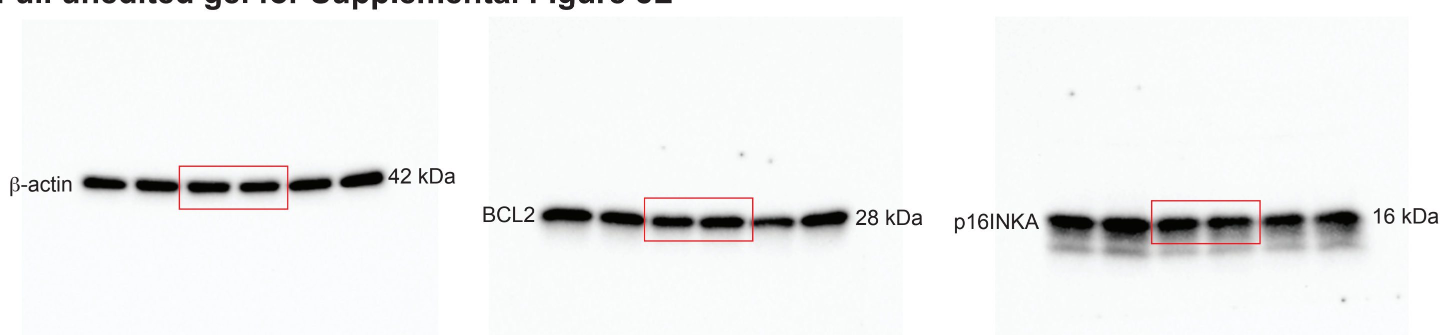

Full unedited gel for Supplemental Figure 9A